

Numerical methods for solving the
time-dependent Schrödinger equation

Bachelor's thesis

Anders Persson

Division of Mathematical Physics

Lund University

Supervisor: Claudio Verdozzi

Co-supervisor: Daniel Karlsson

13 december 2012

Abstract

The main purpose of this thesis is to describe different numerical methods for solving the time-dependent Schrödinger equation. We introduce and describe two different basis representations (spectral and pseudospectral). These basis representations are then used in the different methods we take up for discussion. We consider methods in which the Hamiltonian is constructed in a spectral basis and a pseudospectral basis. We also describe different methods of approximating the time-development of the Hamiltonian. Finally some practical examples will be mentioned.

Contents

1	Introduction	4
2	The time-dependent Schrödinger equation	4
3	Approximation methods	4
3.1	Adiabatic theorem	5
3.2	Adiabatic approximation	5
3.3	Sudden approximation	6
3.4	Dyson series expansion	7
3.5	Magnus expansion	8
3.6	Periodic Hamiltonians and Floquet theory	9
4	Numerical methods	11
4.1	Spectral basis	12
4.2	Pseudospectral basis	12
4.3	Collocation	13
4.4	Gaussian quadrature	16
4.5	Representation of the Hamiltonian in the reduced space	18
4.5.1	The HEG method	19
4.5.2	The DVR method	20
4.6	The Fourier method	23
4.6.1	The FGH method	25
4.6.2	The FFT method	27
4.7	Phase space	28
5	Time propagation	29
5.1	The split operator method	29
5.2	Polynomial methods	30
5.2.1	The Chebyshev method	30
5.2.2	The Lanczos method	31
5.3	The second-order differencing method	34
5.4	The Crank-Nicholson method	35
6	Examples	37
7	Summary	45
8	Appendix	46
8.1	Orthogonal polynomials	46
8.2	Chebyshev polynomials	46
8.3	Discrete Fourier transforms	48
8.4	Morse potential	49

1 Introduction

The subject for this bachelor thesis is to describe different numerical methods for solving the time-dependent Schrödinger equation. A numerical solution of the Schrödinger equation consists of two parts. The first one is an accurate discrete spatial representation of the wave function $\psi(x, t)$. If such a spatial representation is constructed, we can propagate in time an initial wavefunction. Since only a few physical problems can be solved analytically it is important to find numerical methods of solving these equations and also that the methods are not too demanding when it comes to computer capacity. The formal framework for quantum mechanics is as known an infinite-dimensional Hilbert space. So in the numerical calculation we have to truncate this infinite Hilbert space to some N -dimensional Hilbert space, N arbitrary integer. We can express this truncation to N basis by a projection operator P_N . This operator projects onto the space which is spanned by the N -dimensional basis. When it comes to the numerical methods which are used to solve the time-dependent Schrödinger equation. The most common method is to use a grid representation instead of orthogonal bases. When the continuous wavefunction is expressed as a discrete set of time-evolving complex amplitudes at the different grid points we are said to have a grid representation.

2 The time-dependent Schrödinger equation

The main object of this thesis is to describe different numerical methods in solving the time-dependent Schrödinger equation

$$i\hbar \frac{\partial}{\partial t} \Psi(\mathbf{x}, t) = H\Psi(\mathbf{x}, t) \quad (1)$$

Where $H = -\frac{\hbar^2}{2m}\nabla^2 + V$ is the Hamiltonian operator. We have an evolution operator $U(t, t_0)$ which works in the following way $|\Psi(t)\rangle = U(t, t_0) |\Psi(t_0)\rangle$ with $U(t_0, t_0) = \mathbf{1}$. U is defined by

$$i\hbar \frac{\partial}{\partial t} U(t, t_0) = HU(t, t_0) \quad (2)$$

or

$$U(t, t_0) = \mathbf{1} - \frac{i}{\hbar} \int_{t_0}^t HU(t', t_0) dt' \quad (3)$$

If H is hermitian, then $U(t, t_0)$ is a unitary operator.

3 Approximation methods

We now look at different methods which we use to solve the time-dependent Schrödinger equation approximatively. Three approximation cases will be considered. They are all based on the assumption that we can approximate the time-dependent Hamiltonian with a time-independent Hamiltonian over an interval. So on the interval $(t_0, t_0 + \Delta t)$ we have $H(t) \approx H(t_0)$

The first case we look at is when the Hamiltonian changes slowly on the time

scale which are set by the periodic times, which are associated with the approximate stationary solutions. In this case we use adiabatic approximation. In the second the Hamiltonians changes very fast. We then use sudden approximation. To express it in an another way: Say that we denote T as the time during which the modification of the Hamiltonian is done. We suppose that the Hamiltonian is to change-over in a step-wise way. The third is when we split up the Hamiltonian in a time-independent and time-dependent part. In this case a Dyson series expansion is used.

3.1 Adiabatic theorem

We have an initial Hamiltonian H_0 at t_0 and a final Hamiltonian H_1 at t_1 . We infer the following expressions $T = t_1 - t_0$ and $s = (t - t_0)/T$. By $H(s)$ we mean the Hamiltonians value at the time $t = t_0 + sT$. $H(s)$ is a continuous function of s and we have that $H(0) = H_0$ and $H(1) = H_1$. The development of the system from t_0 to t_1 is only dependent on the parameter T , which measures how fast the passage from H_0 to H_1 is. For convenience we infer $U(t, t_0) = U_T(s)$. By $\varepsilon_1 \dots \varepsilon_j$ we denote the eigenvalues of H and the projectors which project onto the associated subspaces is denoted as $P_1 \dots P_j$. All of these quantities are assumed to be continuous functions of s . The subspaces we mention are the vector spaces formed by the eigenstates of $P(s)$ connected to the corresponding eigenvalues. We now state the adiabatic theorem.

Theorem 3.1.1 (Messiah[12])

In the limit when $T \rightarrow \infty$ i.e. in the case of an infinitely slow or adiabatic passage. If the system is initially in an eigenstate of H_0 it will at time t_1 have passed into the eigenstate of H_1 , that derives from it by continuity if

1. The eigenvalues remain distinct throughout the whole transition period $0 \leq s \leq 1$

$$\varepsilon_j(s) \neq \varepsilon_k(s), j \neq k \quad (4)$$

2. The derivatives $\frac{dP_j}{ds}, \frac{d^2P_j}{ds^2}$ are well-defined and piece-wise continuous in the whole interval.

The adiabatic theorem states that if $\Psi(0)$ is an eigenfunction of $H(0)$ and $H(t)$ is a slowly varying function of time, then $\Psi(t)$ will evolve in such a way that it remains an eigenfunction of $H(t)$ for all time.

3.2 Adiabatic approximation

Let us look at a quantum system where we have a discrete structure of levels. The time-dependent Schrödinger equation is

$$i\hbar \frac{\partial}{\partial t} \Psi(x, t) = H(x, t) \Psi(x, t) \quad (5)$$

where

$$H(t) = \begin{pmatrix} \varepsilon_1 & V_{12}(t) & \dots \\ V_{21}(t) & \varepsilon_2 & \dots \\ \dots & \dots & \ddots \end{pmatrix}$$

and

$$\Psi(t) = \begin{pmatrix} \Psi_1 \\ \Psi_2 \\ \vdots \end{pmatrix}$$

and finally $V(t)$ is the off-diagonal couplings. If it is the case that the off-diagonal couplings are slowly varying, we have that some conclusions can be made. We continue by defining the unitary transformation which diagonalizes $H(t)$.

$$U^{-1}(t)H(t)U(t) = D(t) \quad (6)$$

and infer $U^{-1}\Psi \equiv \Psi'$. The time-dependent Schrödinger equation becomes

$$i\hbar \frac{\partial}{\partial t}(U\Psi'(t)) = i\hbar(U(t)\frac{\partial\Psi'}{\partial t} + \frac{\partial U(t)}{\partial t}\Psi') = H(t)U(t)\Psi'(t) \quad (7)$$

or

$$i\hbar \frac{\partial}{\partial t}\Psi'(t) = D(t)\Psi'(t) - i\hbar U^{-1}(t)\frac{\partial U(t)}{\partial t}\Psi'(t) \quad (8)$$

By this we see that if $H(t)$ is slowly varying, $U(t)$ and $U^{-1}(t)$ will also be slowly varying. If we ignore the second term on the right side of (8), we have what is called adiabatic approximation. We note that we get a system of uncoupled differential equations, which do not demand so much computer capacity.

To give an concrete example. We have a charged-particle linear harmonic oscillator acted upon by a spatially uniform time-dependent electric field $E(t)$. The Hamiltonian of the system is

$$H(t) = -\frac{\hbar^2}{2m} \frac{\partial^2}{\partial x^2} + \frac{1}{2}kx^2 - qE(t)x$$

where m is the mass and q is the charge of the particle and the perturbation $qE(t)x$ is assumed to be switched on at $t = t_0$ and switched off at $t = t_1$ in a smooth way. This means that the particles at the end of the time-evolution will be in the ground state. To give a classical example of adiabatic approximation, let us consider a pendulum that is transported around near the surface of the earth. The pendulum will behave normally as you climb a mountain with only the period slowly lengthening as the force of gravity decreases so long as the time over which the height is changed is long compared to the pendulum period.

3.3 Sudden approximation

As mentioned before the Hamiltonians in this case change very fast. We shall express it now more formally. Let's consider the Schrödinger equation for the time-evolution operator

$$i\hbar \frac{\partial}{\partial t}U(t, t_0) = HU(t, t_0) \quad (9)$$

This expression can be expressed in the following way

$$i \frac{\partial}{\partial s}U(t, t_0) = \frac{H}{\hbar/T}U(t, t_0) = \frac{H}{\hbar\Omega}U(t, t_0) \quad (10)$$

where time is expressed as $t = sT$, where s is a dimensionless parameter and a time scale T . We infer the following definition $\Omega \equiv \frac{1}{T}$. In the sudden approximation we have that if $T \rightarrow 0$ then $\hbar\Omega$ will become considerable larger than the energy scale which is represented by H under the assumption that by adding or subtracting an arbitrary constant we can change H and in the statevector introduce an overall phase factor. We have that $U(t, t_0) \rightarrow 1$ as $T \rightarrow 0$. Which gives the validity of the sudden approximation. To be more explicit we have before and after the rapid change

$$U(t, t_0) = e^{\frac{i}{\hbar}Ht}, t < t_0$$

$$U(t, t_0) = e^{\frac{i}{\hbar}H't}, t > t_0$$

We have approximated $H(t)$ by an stepfunction. The usefulness of sudden approximation can be seen in the following way

$$U(t, t_0) = T e^{\frac{i}{\hbar} \int H'(t') dt'} = T e^{\frac{i}{\hbar} H' \int dt'} = e^{\frac{i}{\hbar} H' (t-t_0)}$$

where T is a time-ordering operator and $t > t_0$. We get a much more simple expression which does not demand so much computer capacity.

As an example where sudden approximation can be used is for instance when we have an atom in a constant magnetic field when the direction of the magnetic field is suddenly reversed. Another example is the charged-particle linear harmonic oscillator mentioned in the section about adiabatic approximation. We can use sudden approximation if say at $t = 0$ the electric field is switched on suddenly and afterwards it is assumed that it has a constant value E_0 .

3.4 Dyson series expansion

We have a Hamiltonian that can be divided in two parts $H = H_0 + V(t)$ where $V(t)$ is a time-dependent potential and $H_0 | n \rangle = E_n | n \rangle$. We say that at $t = 0$, the state ket is given by

$$| \alpha \rangle = \sum_n c_n(0) | n \rangle \quad (11)$$

We want $c_n(t)$ for $t > 0$ to fulfill

$$| \alpha, t_0 = 0; t \rangle = \sum_n c_n(t) e^{-iE_n t/\hbar} | n \rangle \quad (12)$$

We are here in the Schrödinger picture. We now continue in the interaction picture. We know that

$$| \alpha, t_0; t \rangle_I = e^{iH_0 t/\hbar} | \alpha, t_0; t \rangle_S \quad (13)$$

where I stands for the interaction picture and S for the Schrödinger picture.

The time derivate of this expression with $H = H_0 + V(t)$ gives

$$i\hbar \frac{\partial}{\partial t} | \alpha, t_0; t \rangle_I = V_I | \alpha, t_0; t \rangle_I \quad (14)$$

We continue by performing the following expansion

$$| \alpha, t_0; t \rangle_I = \sum_n c_n(t) | n \rangle \quad (15)$$

By multiplying by $\langle n |$ we get the following differential equation

$$i\hbar \frac{d}{dt} c_n(t) = \sum_m V_{nm} e^{i\omega_{nm}t} c_m(t) \quad (16)$$

where

$$\omega_{nm} = \frac{(E_n - E_m)}{\hbar} = -\omega_{mn} \quad (17)$$

and E_n, E_m are energy eigenvalues. With some few exceptions exact solutions for $c_n(t)$ are not available. So we have to use an approximate solution which is obtained by perturbation expansion.

$$c_n(t) = c_n^{(0)} + c_n^{(1)} + c_n^{(2)} \dots \quad (18)$$

where we by $c_n^{(1)}, c_n^{(2)} \dots$ mean amplitudes in the strength parameter of the time-dependent potential of first order, second order and so on.

Another way is to use the time-evolution operator defined in the interaction picture as

$$| \alpha, t_0; t \rangle_I = U_I(t, t_0) | \alpha, t_0; t_0 \rangle_I \quad (19)$$

We have then the following differential equation

$$i\hbar \frac{d}{dt} U_I(t, t_0) = V_I(t) U_I(t, t_0) \quad (20)$$

with the initial condition

$$U_I(t_0, t_0) = 1 \quad (21)$$

This can be written as an integral equation

$$U_I(t, t_0) = 1 - \frac{i}{\hbar} \int_{t_0}^t V_I(t') U_I(t', t_0) dt' \quad (22)$$

The approximate solution to this equation by the help of iteration is called a Dyson series.

$$\begin{aligned} U_I(t, t_0) &= 1 - \frac{i}{\hbar} \int_{t_0}^t V_I(t') [1 - \frac{i}{\hbar} \int_{t_0}^{t'} V_I(t'') U_I(t'', t_0) dt''] dt' \quad (23) \\ &= 1 - \frac{i}{\hbar} \int_{t_0}^t dt' V_I(t') + (\frac{-i}{\hbar})^2 \int_{t_0}^t dt' \int_{t_0}^{t'} dt'' V_I(t') V_I(t'') \\ &+ \dots + (\frac{-i}{\hbar})^n \int_{t_0}^t dt' \int_{t_0}^{t'} dt'' \dots \int_{t_0}^{t^{(n-1)}} dt^{(n)} V_I(t') V_I(t'') \dots V_I(t^n) + \dots \end{aligned}$$

where the truncated sum of (23) is used in the approximation.

3.5 Magnus expansion

This expansion is an alternative to time-dependent perturbation theory. The reason why it is used is that we can truncate the Magnus expansion at any order and despite of this have a unitary expression for the propagator. The Magnus expansions gives an expression for the propagator for time-dependent Hamiltonians as the exponential of an infinite sum of operators. We can at any arbitrary order truncate the infinite sum in the exponent. This gives an approximation to the propagator. We start with presenting a formal way of expressing the integral representation for time-dependent Hamiltonians. It has the following form

$$\Psi(x, t) = T e^{-i \int_0^t H(t') dt' / \hbar} \Psi(x, 0) \quad (24)$$

where T is the time-ordering operator which by its definition put in the Taylor series the operators in their chronological order. We would like to write the propagator in the following form $U(t, 0) = e^{A(t)}$, where $A(t) = A_1(t) + A_2(t) + \dots$. This is done by the Magnus expansion. So we get the following form of the first A:s

$$\begin{aligned} A_1 &= \frac{1}{i\hbar} \int_0^t dt_1 H(t_1) \\ A_2 &= -\frac{1}{2} \left(\frac{1}{i\hbar}\right)^2 \int_0^t dt_2 \int_0^{t_2} dt_1 [H(t_1), H(t_2)] \\ A_3 &= -\frac{1}{6} \left(\frac{1}{i\hbar}\right)^3 \int_0^t dt_3 \int_0^{t_3} dt_2 \int_0^{t_2} dt_1 [H(t_1), [H(t_2), H(t_3)]] \\ &\quad + [[H(t_1), H(t_2)], H(t_3)] \end{aligned}$$

and so on.

We have that the higher-order terms in the Magnus expansion as seen above involve sums of integrals.

3.6 Periodic Hamiltonians and Floquet theory

We consider in this section Hamiltonians which are periodic in time. The theory of the systems in this case is called Floquet theory.

We start our investigation with the time-dependent Schrödinger equation

$$i\hbar \frac{\partial}{\partial t} \Psi(x, t) = H(x, t) \Psi(x, t) \quad (25)$$

where the Hamiltonian is periodic with period T or in a more formal way $H(x, t+T) = H(x, t)$.

We infer the following trial form

$$\Psi_\lambda(x, t) = e^{-i\varepsilon_\lambda t/\hbar} \Phi_\lambda(x, t) \quad (26)$$

If we insert (26) in the time-dependent Schrödinger equation and infer the following definition

$$H_F(x, t) \equiv \left(H(x, t) - i\hbar \frac{\partial}{\partial t} \right) \quad (27)$$

where H_F denotes the Floquet Hamiltonian, H_F is hermitian, we get after some algebra

$$H_F(x, t) \Phi_\lambda(x, t) = \varepsilon_\lambda \Phi_\lambda(x, t) \quad (28)$$

Here $\Phi_\lambda(x, t)$ is denoted as a Floquet eigenstate. This equation is an eigenvalue equation in the variables, x and t , where the time-independent eigenvalues are the Floquet energies ε_λ . One result worth mentioning is that the Floquet eigenstates $\Phi_\lambda(x, t)$ and the Hamiltonian have equal period T . The general solution to the time-dependent Schrödinger equation are

$$\Psi(x, t) = \sum_\lambda a_\lambda e^{-i\varepsilon_\lambda t/\hbar} \Phi_\lambda(x, t) \quad (29)$$

and $\Psi_\lambda(x, t)$ is a representation of a particular Ψ solution to the time-dependent Schrödinger equation.

We can get another formulation which is based on the terms of basis sets in space and time if we rewrite $\Psi_\lambda(x, t)$ in the following way

$$\Psi_\lambda(x, t) = e^{-i\varepsilon_\lambda t/\hbar} \Phi_\lambda(x, t) = e^{-i(\varepsilon_\lambda + n\hbar w)t/\hbar} e^{inwt} \Phi_\lambda(x, t) \quad (30)$$

We now get a new series of Floquet eigenvalues. These eigenvalues have the following form $\varepsilon_\lambda + n\hbar w$ and the eigenfunctions are $\Phi_{\lambda n}(x, t) = e^{inwt} \Phi_\lambda(x, t)$. In the case when n is an integer, $\Phi_{\lambda n}(x, t)$ will be periodic in t if $\Phi_\lambda(x, t)$ also is periodic in t for specific values of w . We have that the physical state $\Psi_\lambda(x, t)$ has not changed and because of that the Floquet eigenvalues which are associated with distinct physical states are accordingly defined modulo $\hbar w$.

Let us now define a composite Hilbert space in position and time $R \oplus T$. The temporal part is spanned by the complete orthonormal set of Fourier functions e^{inwt} , where $-\infty < n < \infty$, n is an integer. With the help of square-integrable functions in the configuration space we span the spatial part. We have that the Floquet eigenstates fulfill the following orthonormality condition

$$\langle\langle \Phi_{\kappa n} | \Phi_{\nu m} \rangle\rangle = \frac{1}{T} \int_0^T dt \int_{-\infty}^{\infty} dx \Phi_{\kappa n}^*(x, t) \Phi_{\nu m}(x, t) = \delta_{\kappa\nu} \delta_{nm} \quad (31)$$

The Floquet eigenstates forms a complete set in $R \oplus T$:

$$\sum_{\kappa n} | \Phi_{\kappa n} \rangle \rangle \langle\langle \Phi_{\kappa n} | = \mathbf{1} \quad (32)$$

We stop here and notice that we have a new notation. This notation is called the double bra-ket notation here used to denote the inner product over x and t . We continue now with the question how to represent the Floquet Hamiltonian in an arbitrary complete basis. We infer the following expression $| \alpha n \rangle \rangle \equiv | \alpha \rangle | n \rangle$, where $| n \rangle$ are Fourier vectors which fulfills the following equation $\langle t | n \rangle = e^{inwt}$ and $| \alpha \rangle$ are eigenstates that solve the following equation

$$H(x)\alpha(x) = E_\alpha^0 \alpha(x) \quad (33)$$

We have that $H(x, t)$ and $\Phi_\lambda(x, t)$ are periodic in time and because of that can we expand them in Fourier series

$$\int_{-\infty}^{\infty} \beta^*(x) \Phi_\lambda(x, t) dx = \sum_{m=-\infty}^{\infty} \phi_{\beta\lambda}^{(m)} e^{imwt} \quad (34)$$

and

$$\int_{-\infty}^{\infty} \alpha^*(x) H(x, t) \beta(x) dx = \sum_{n=-\infty}^{\infty} H_{\alpha\beta}^{(n)} e^{inwt} \quad (35)$$

The expansions above can be inserted into the Schrödinger equations and the result is the following infinite set of relations for $\phi_{\alpha\lambda}^{(n)}$:

$$\sum_{\beta m} \langle\langle \alpha n | \tilde{H}_F | \beta m \rangle\rangle \phi_{\beta\lambda}^{(m)} = \varepsilon_\lambda \phi_{\alpha\lambda}^{(n)} \quad (36)$$

where we by \tilde{H}_F denote the time-independent Floquet Hamiltonian with the following matrix elements

$$\langle\langle \alpha n | \tilde{H}_F | \beta m \rangle\rangle = H_{\alpha\beta}^{(n-m)} + n\hbar w \delta_{\alpha\beta} \delta_{nm} \quad (37)$$

The structure of the matrix is as follows, where n goes between -2 and 2.

$$[H_F] = \begin{pmatrix} \mathbf{A} + 2w\mathbf{I} & \mathbf{B} & 0 & 0 & 0 \\ \mathbf{B} & \mathbf{A} + w\mathbf{I} & \mathbf{B} & 0 & 0 \\ 0 & \mathbf{B} & \mathbf{A} & \mathbf{B} & 0 \\ 0 & 0 & \mathbf{B} & \mathbf{A} - w\mathbf{I} & \mathbf{B} \\ 0 & 0 & 0 & \mathbf{B} & \mathbf{A} - 2w\mathbf{I} \end{pmatrix}$$

where \mathbf{A} consists of the matrix elements of the time-averaged Hamiltonian, \mathbf{B} consists of the Fourier component at the frequency w of the coupling between the basis functions. These basis functions are induced by the periodic Hamiltonian. The following expression gives the matrix \mathbf{A}

$$A_{\alpha\beta} = \langle\langle \alpha 0 | H(x, t) | \beta 0 \rangle\rangle = \frac{1}{T} \int_0^T \langle \alpha | H(x, t) | \beta \rangle dt = \langle \alpha | \bar{H}(x) | \beta \rangle \quad (38)$$

where we by $\bar{H}(x)$ mean the time average of $H(x, t)$.

If $H(x, t) = H_0(x) + V(x, t)$ and $\bar{V}(x) = 0$. The time-averaged Hamiltonian is the system $H_0(x)$. We can choose the basis functions (α, β) to be eigenstates of $\bar{H}(x)$. In this case \mathbf{A} is diagonal.

The following expression gives the matrix \mathbf{B}

$$B_{\alpha\beta} = \langle\langle \alpha 0 | H(x, t) | \beta 1 \rangle\rangle = \frac{1}{T} \int_0^T \langle \alpha | H(x, t) | \beta \rangle e^{i\omega t} dt \quad (39)$$

We now turn to the question of diagonalization of the matrix. We have that the number of eigenvalues of the Floquet matrix is infinite, but the periodicity gives that if ε_λ is an eigenvalue so is also $\varepsilon_\lambda + n\hbar w \equiv \varepsilon_{\lambda n}$ for any integer n . In a similar way, even though the eigenvectors are distinct in $R \oplus T$ they are connected by the periodicity relationship

$$\langle\langle \alpha, n + p | \Phi_{\lambda, m+p} \rangle\rangle = \langle\langle \alpha, n | \Phi_{\lambda, m} \rangle\rangle \quad (40)$$

So by a phase factor $e^{ip\omega t}$ the basis functions differ in the bra from the basis functions in the ket if we combine the basis function with the Floquet eigenvalue which they are associated with. They are generators for equal dynamics. So we have that the formally infinite number of eigenvalues and eigenfunctions which come from the diagonalization of the infinite Floquet matrix can be reduced to N distinct eigenvalues and N eigenfunctions, all of them physically distinct. N is the number of basis functions of $\bar{H}(x)$, which comes from the periodicity relations.

So using a complete basis in both position and time gives a representation of the Hamiltonian that is time independent. This allows the use of all the theorems and techniques of time-independent Hamiltonians to periodic time-dependent Hamiltonians.

4 Numerical methods

We come now to the main part of the thesis, where we take up the spatial part and other topics mentioned in the introduction and some not mentioned. The spectral and pseudospectral basis, collocation, Gaussian quadrature, the

HEG(Harris. Engerholm and Gwinn) method, The DVR(Discrete Variable Representation) method. In the end of this section we take up for discussion the Fourier method and the implement of this method, the FGH(Fourier Grid Hamiltonian) method and the FFT(Fast Fourier Transform) method.

4.1 Spectral basis

With a spectral basis we mean a basis of orthogonal functions. We must truncate this infinite set of orthogonal functions at some arbitrary finite value N . We use a projection operator for this purpose.

$$P_N = \sum_{n=1}^N |\phi_n\rangle\langle\phi_n| \quad (41)$$

Let us now look at how the spectral projection operator acts on a wavefunction. Start with an arbitrary wavefunction $\psi(x)$. Which we express in an orthonormal basis (ϕ_n) in the following way

$$\psi(x) = \sum_{n=1}^{\infty} a_n \phi_n(x) \quad (42)$$

where

$$\int \phi_m^*(x) \phi_n(x) dx = \delta_{mn}, \quad (43)$$

and

$$a_n = \int \phi_n^*(x) \psi(x) dx \quad (44)$$

where $m, n = 1, \dots, \infty$

The spectral projection operator P_N is defined so that

$$\tilde{\psi}(x) = P_N \psi(x) = \sum_{n=1}^N a_n \phi_n(x) \quad (45)$$

where a_n is given in equation(44) for $n = 1, \dots, N$

We have then

$$\begin{aligned} P_N \phi_n(x) &= \phi_n(x), n = 1, \dots, N \\ P_N \phi_n(x) &= 0, n = N + 1, \dots \end{aligned} \quad (46)$$

4.2 Pseudospectral basis

It is known that an operator is basis independent and can therefore be represented in other basis then the spectral basis. We will later many times mention what is called a pseudospectral basis, which is a basis of spatially localized functions. Each of these functions is concentrated at different spatial centers. We denote these pseudospectral basis functions as (θ_j) . The N pseudospectral basis functions and the N spectral basis functions span the same Hilbert space and are connected to each other through a unitary transformation. So we have

$$P_N = \sum_{n=1}^N |\phi_n\rangle\langle\phi_n| = \sum_{j=1}^N |\theta_j\rangle\langle\theta_j| \quad (47)$$

4.3 Collocation

Collocation or pseudospectral approximation can be described in the following way. We use a projection operator defined in the following way

$$\tilde{\psi}(x) = P_N \psi(x) = \sum_{n=1}^N b_n \phi_n(x) \quad (48)$$

where the condition

$$\tilde{\psi}(x) = \psi(x) \quad (49)$$

at the collocation points (x_i) , $i = 1, \dots, N$ determine b_n . So we have

$$\tilde{\psi}(x_i) = P_N \psi(x_i) = \sum_{n=1}^N b_n \phi_n(x_i) = \psi(x_i) \quad (50)$$

where $i = 1, \dots, N$.

This equation can be used as an interpolation scheme at points which are not collocation points through the relation

$$\tilde{\psi}(x) = \sum_{n=1}^N b_n \phi_n(x) \approx \psi(x) \quad (51)$$

One observation which can be made is that P_N in the case of spectral projection and in the case of collocation projects onto the subspace which we denote as $\Xi_N \equiv \text{span}(\phi_1, \dots, \phi_N)$ of the Hilbert space. The difference between the two types of projectors is not the subspace which they are projected onto but in the state in the reduced subspace expressed in terms of the difference between the coefficients (a_n) and (b_n) . We can express this difference in the state by the help of geometry. For details see (Tannor[17]). The result is that the spectral projector is an orthogonal projector and the collocation projector is a nonorthogonal projector. One question which comes to mind is the following, if we have a projector which fulfills the collocation conditions. Is it possible for it to be an orthogonal projector at the same time? We consider first the case where the following discrete orthogonality relation at the collocation points

$$\sum_{j=1}^N \phi_m^*(x_j) \phi_n(x_j) \Delta_j = \delta_{mn} \quad (52)$$

where $m, n = 1, \dots, N$ and Δ_j is a generally j -dependent weight factor is fulfilled by the expansion functions $\phi_n(x)$. The points x_j and weights Δ_j have to fulfill all the orthogonality relations for $1 \leq m, n \leq N$.

We have that equation(52) permits for the use of direct inversion of the coefficients b_n in the expression $\psi(x_i) = \sum_{n=1}^N b_n \phi_n(x_i)$ by multiplying from the left with $\phi_m^*(x_j) \Delta_j$ and by summing over j , so we have

$$b_n = \sum_{j=1}^N \psi(x_j) \phi_n^*(x_j) \Delta_j \quad (53)$$

with (b_n) chosen in this way the collocation conditions are fulfilled. This expression is a discrete approximation to

$$a_n = \int \phi_n^*(x)\psi(x)dx \quad (54)$$

which is the condition for an orthogonal projection. We will call these schemes satisfying $\sum_{j=1}^N \phi_m^*(x_j)\phi_n(x_j)\Delta_j = \delta_{mn}$ where $m, n = 1 \dots N$ for orthogonal collocation schemes. If we infer the following definition

$$\Phi_n(x_j) = \sqrt{\Delta_j}\phi_n(x_j) \quad (55)$$

the discrete orthogonality relations at the collocation points becomes

$$\sum_{j=1}^N \Phi_m^*(x_j)\Phi_n(x_j) = \delta_{mn} \quad (56)$$

where $1 \leq m, n \leq N$.

If we define $\Phi_n(x_j) \equiv \Phi_{jn}$. The equation (56) becomes in matrix notation

$$\Phi^\dagger \Phi = \mathbf{1} \quad (57)$$

Relations of this form is denoted as basis orthogonality relations. The form gives an indication that Φ , the transformation matrix is unitary. So because of this we have that

$$\Phi \Phi^\dagger = \mathbf{1} \quad (58)$$

Relations of this form are denoted as grid orthogonality relations. This relation expressed in components becomes

$$\sum_{n=1}^N \Phi_n(x_i)\Phi_n^*(x_j) = \delta_{ij} \quad (59)$$

for $1 \leq i, j \leq N$

The pseudospectral basis can be derived from orthogonal collocation (for details see Tannor[17]). The result is the following definition for the pseudospectral basis functions

$$\sum_{n=1}^N \phi_n(x)\Phi_n^*(x_j) \equiv \theta_j(x) \quad (60)$$

The functions denoted as the pseudospectral basis functions ($\theta_j(x)$) are localized around different values of x_j . They fulfill the following condition called the modified Kronecker δ -function property

$$\theta_j(x_i) = \frac{\delta_{ij}}{\sqrt{\Delta_j}} \quad (61)$$

We can express the pseudospectral basis functions in matrix-vector notation and get

$$\Phi^\dagger \phi(x) = \theta(x) \quad (62)$$

which shows that we can consider the functions ($\theta_j(x)$) as an alternative basis to (ϕ_n) since (θ_j) and (ϕ_n) are related through a unitary transformation Φ^\dagger .

This gives that a projection in respective basis projects onto a subspace of the Hilbert space which is the same in both cases. So the unitary collocation relation of the following form $\sum_{j=1}^N \Phi_m^*(x_j) \Phi_n(x_j) = \delta_{mn}$ gives that we have a set of localized basis functions. These functions span the space which is spanned by the orthogonal functions. The points and weights in equation(59) and the basis of orthogonal functions (ϕ_n) determine the localized basis

Let us now consider the completeness and orthogonality of the localized basis functions (θ_n). We multiply the pseudospectral basis functions by $\phi_m^*(x)$ and then integrate over the domain and get

$$\Phi_n^*(x_j) = \langle \phi_n | \theta_j \rangle \quad (63)$$

so the grid orthogonality relation is

$$\sum_{n=1}^N \Phi_n(x_i) \Phi_n^*(x_j) = \delta_{ij} = \sum_{j=1}^N \langle \theta_i | \phi_n \rangle \langle \phi_n | \theta_j \rangle = \langle \theta_i | \theta_j \rangle \quad (64)$$

which is a description of the different θ basis functions orthonormality and the basis orthogonality relation is

$$\sum_{j=1}^N \Phi_m^*(x_j) \Phi_n(x_j) = \delta_{mn} = \sum_{j=1}^N \langle \phi_m | \theta_j \rangle \langle \theta_j | \phi_n \rangle \quad (65)$$

The orthogonality and completeness of the θ function is a consequence of the fact that the transformation matrix is unitary.

Let us now look at the collocation relation. The definition for the pseudospectral basis functions can be expressed as

$$\phi_n(x) = \sum_{i=1}^N \Phi_n(x_i) \theta_i(x) \quad (66)$$

which in matrix-vector notation becomes

$$\Phi \theta(x) = \phi(x) \quad (67)$$

We can use this relation to express the collocation relation with the help of $\Phi_n(x_j) = \sqrt{\Delta_j} \phi_n(x_j)$ and $\tilde{\psi}(x_i) = \sum_{n=1}^N b_n \phi_n(x_i) = \psi(x_i)$ and get

$$\tilde{\psi}(x_i) = \sum_{n=1}^N b_n \phi_n(x) = \sum_{i=1}^N \left(\sum_{n=1}^N b_n \Phi_n(x_i) \right) \theta_i(x) \quad (68)$$

$$= \sum_{i=1}^N \psi(x_i) \theta_i(x) \sqrt{\Delta_i} \approx \psi(x) \quad (69)$$

We have at the collocation points (x_i) the following relation

$$\tilde{\psi}(x_i) = \sum_{i=1}^N \psi(x_i) \theta_i(x_i) \sqrt{\Delta_i} = \psi(x_i) \quad (70)$$

If we compare this expression with $\tilde{\psi}(x_i) = \sum_{n=1}^N b_n \phi_n(x_i) = \psi(x_i)$, we notice that this expression is a collocation formula with basis functions (θ_i) instead of

(ϕ_n). At the collocation points (x_i) are the values of the exact function $\psi(x)$ coefficients of the basis functions.

We continue by multiplying the collocation relation with $\theta_j(x)$ and integrate. Then we have

$$\langle \theta_j | \tilde{\psi} \rangle = \sum_{i=1}^N \psi(x_i) \langle \theta_j | \theta_i \rangle \sqrt{\Delta_i} = \psi(x_j) \sqrt{\Delta_j} \quad (71)$$

The collocation projector has the following expression in the Dirac notation.

$$\langle x | \tilde{\psi} \rangle = \sum_{i=1}^N \psi(x_i) \theta_i(x) \sqrt{\Delta_i} = \sum_{i=1}^N \langle x | \theta_i \rangle \langle x_i | \psi \rangle \sqrt{\Delta_i} \quad (72)$$

We have also $\langle x | \tilde{\psi} \rangle = \langle x | P_N | \psi \rangle$ so we can write the collocation projector as

$$P_N = \sum_{i=1}^N | \theta_i \rangle \langle x_i | \sqrt{\Delta_i} \quad (73)$$

4.4 Gaussian quadrature

We will now describe the theory of Gaussian quadrature. Let us consider

$$\int_a^b w(x) f(x) dx \approx \sum_{i=1}^N W_i f(x_i) \quad (74)$$

where the values (W_i) are the weights which are given to the function values $f(x_i)$ and $w(x)$ is a positive weight function. We choose (x_i) and (W_i) so that if $f(x)$ is a polynomial of degree $2N - 1$ or less the sum in equation(74) gives the integral exactly. We consider now the following set of polynomials ($p_n, n = 0, \dots, N - 1$) fulfilling the following orthogonality relation

$$\int_a^b w(x) p_m(x) p_n(x) dx = \delta_{mn} \quad (75)$$

If we choose the points and weights in accordance with an N -point Gaussian quadrature. The approximation in equation(74) will be an equality for polynomials up to an degree of $2N - 1$. So we have

$$\int_a^b w(x) p_m(x) p_n(x) dx = \sum_{i=0}^{N-1} W_i p_m(x_i) p_n(x_i) = \delta_{mn} \quad (76)$$

We define the function

$$\phi_n(x) = \sqrt{w(x)} p_n(x) \quad (77)$$

and the matrix Φ with the following elements

$$\phi_{in} = \sqrt{W_i} p_n(x_i) \quad (78)$$

So equation(76) becomes in matrix form

$$\Phi^\dagger \Phi = \mathbf{1} \quad (79)$$

which shows that Φ is unitary.

Let us consider $\int_a^b w(x)p_m(x)p_n(x)dx$ which is a polynomial of an degree no higher than $2N - 1$, which gives that the Gaussian quadrature has to be exact.

$$\begin{aligned} \int_a^b w(x)p_m(x)p_n(x)dx &= \sum_{i=0}^{N-1} W_i p_m(x_i) p_n(x_i) \\ &= \sum_{i,j=0}^{N-1} \Phi_{mi}^\dagger x_{ij} \Phi_{jn} = X_{mn} \end{aligned} \quad (80)$$

which in matrix notation becomes

$$\mathbf{X} = \Phi^\dagger \mathbf{x} \Phi \quad (81)$$

where we have that \mathbf{x} is a diagonal matrix with elements x_{ij} and \mathbf{X} is an $N \times N$ matrix with elements X_{mn} defined in equation(80). The splitting of the matrix \mathbf{X} in three matrices is unique and we have that Φ_{in} has to fulfill $\Phi_{in} = \sqrt{w_i} p_n(x_i)$ and x_{ii} is the i :th Gaussian quadrature node. The splitting of \mathbf{X} gives a procedure for finding Gaussian quadrature points and weights. This procedure is called the HEG(Harris, Engerholm and Gwinn) algorithm. By using the first N basis functions can we construct an $N \times N$ matrix representation \mathbf{X} of the \hat{x} operator.

$$X_{mn} = \int_a^b \phi_m(x)x\phi_n(x)dx = \int_a^b w(x)p_m(x)p_n(x)dx \quad (82)$$

Because of the three-term recursion relation fulfilled by orthogonal polynomials (see Bau and Trefethen[3]), we have that the matrix \mathbf{X} is tridiagonal. \mathbf{X} is thereafter diagonalized by a unitary transformation

$$\mathbf{U}^{-1} \mathbf{X} \mathbf{U} = \Phi \mathbf{X} \Phi^\dagger = \mathbf{x} \quad (83)$$

The integration points of equation (80) are the eigenvalues (x_i) and this gives that the eigenvalues (x_i) also are Gaussian quadrature points of $\int_a^b w(x)f(x)dx \approx \sum_{i=1}^N W_i f(x_i)$. From the first row of the matrix $\mathbf{U} = \Phi^\dagger$ (first column of Φ) we can get the weights after we have looked at the orthogonal collocation matrix where the points and weights are based on Gaussian quadrature. We continue with the corresponding pseudospectral functions. One observation to be made from

$$\Phi \mathbf{X} \Phi^\dagger = \mathbf{U}^{-1} \mathbf{X} \mathbf{U} = \mathbf{x}$$

is that the eigenvectors of \mathbf{X} are the columns of Φ^\dagger . So the eigenfunctions of \hat{x}_N are

$$\theta_i(x) = \sum_{n=1}^N \Phi_{ni}^\dagger \phi_n(x) \quad (84)$$

where $\Phi_{ni}^\dagger = \langle \phi_n | \theta_i \rangle$

This is as seen the definition of a pseudoscalar basis function. So (θ_i) can be expressed as a linear combination of delocalized spectral basis functions. So the localized pseudospectral functions must in this case also be the mentioned

linear combinations. The Gaussian quadrature pseudospectral functions is of the following form

$$\theta_j(x) = \sum_{n=1}^N \phi_n(x) \Phi_n^*(x_j) = \sum_{n=1}^N \sqrt{w(x)} p_n(x) \sqrt{W_j} p_n(x_j) \quad (85)$$

A comparison with the grid orthogonality relation

$$\sum_{n=1}^N \sqrt{W_i} p_n(x_i) \sqrt{W_j} p_n(x_j) = \delta_{ij} \quad (86)$$

gives

$$\left(\frac{W_i}{w(x_i)}\right)^{1/2} \theta_j(x_i) = \delta_{ij} \quad (87)$$

We continue by expressing X_{mn} in Dirac notation

$$X_{mn} = \langle \phi_m | \hat{x} | \phi_n \rangle = \langle \phi_m | P_N \hat{x} P_N | \phi_n \rangle \quad (88)$$

We can insert the orthogonal projection operator P_N because ϕ_n and ϕ_m are not affected by this operator. For simplicity and later use we define the operator as

$$\hat{x}_N = P_N \hat{x} P_N \quad (89)$$

The ij :th element of $\Phi \mathbf{X} \Phi^\dagger$ can be expressed as

$$\begin{aligned} \sum_{m,n=1}^N \langle \theta_i | \phi_m \rangle \langle \phi_m | \hat{x}_N | \phi_n \rangle \langle \phi_n | \theta_j \rangle \\ = \langle \theta_i | \hat{x}_N | \theta_j \rangle = x_i \delta_{ij} \end{aligned} \quad (90)$$

which shows that in a basis independent representation, the eigenfunctions of the projected \hat{x} operator, \hat{x}_N are the localized pseudospectral functions. The eigenvalue equation have in the coordinate representation the following form

$$\hat{x}_N \theta_i(x) = x_i \theta_i(x) \quad (91)$$

4.5 Representation of the Hamiltonian in the reduced space

Now it comes to the projectors we have mentioned earlier. We have mainly studied their effect on wavefunctions. We now turn our attention to constructing the Hamiltonian operator $H = T(\hat{p}) + V(\hat{x})$ by the help of these projectors. Since it is convenient to evaluate the kinetic energy T_N in a spectral basis and the potential energy V_N in a pseudospectral basis. Because of this a single representation has to be chosen for the Hamiltonian. This can be done if the unitary transformation between the two bases is known. The equivalence of the projection operators in the two representations gives that the reduced Hilbert space on which the Hamiltonian is represented is defined in a consistent way. We will describe the construction of the Hamiltonian in a spectral basis, $P_N = \sum_{n=1}^N | \phi_n \rangle \langle \phi_n |$ and in a pseudospectral basis, $P_N = \sum_{i=1}^N | \theta_i \rangle \langle \theta_i |$

4.5.1 The HEG method

We start with considering a Hamiltonian of the following form

$$H = \hat{p}^2/2m + V(\hat{x}) = T(\hat{p}) + V(\hat{x}) \quad (92)$$

We use spectral projection on the full Hilbert space to get an N -dimensional Hilbert space. We express the truncated operators as

$$H_N = P_N T(\hat{p}) P_N + P_N V(\hat{x}) P_N \quad (93)$$

where

$$P_N = \sum_{n=1}^N |\phi_n\rangle\langle\phi_n| \quad (94)$$

From this we have that the matrix elements become

$$\langle\phi_n | T(\hat{p}) | \phi_m\rangle \quad (95)$$

and

$$\langle\phi_n | V(\hat{x}) | \phi_m\rangle \quad (96)$$

For simplicity we consider a one-dimensional description. In the spectral representation let us consider $T = \hat{p}^2/2m$ then we have

$$T_{mn} = \langle\phi_m | T | \phi_n\rangle = -\frac{\hbar^2}{2m} \int_a^b \phi_m^*(x) \frac{\partial^2}{\partial x^2} \phi_n(x) dx \quad (97)$$

so we have an analytic expression which can often be solved analytically. This is not the case when it comes to the potential energy matrix elements in the spectral representation.

$$V_{mn} = \langle\phi_m | V(\hat{x}) | \phi_n\rangle = \int_a^b \phi_m^*(x) V(x) \phi_n(x) dx \quad (98)$$

As seen before can we use Gaussian quadrature to get an approximation consisting of a finite sum of the integral of the function $f(x)$. This approximation is of the form $\int_a^b w(x) f(x) dx \approx \sum_{i=1}^N W_i f(x_i)$, and by using $\phi_l(x) = \sqrt{w(x)} p_l(x)$ where $l = m, n$ we see that we have $f(x) = p_n(x) V(x) p_m(x)$ in the quadrature formula and we get for the individual matrix elements

$$V_{mn} \approx \sum_{i=1}^N W_i p_m(x_i) V(x_i) p_n(x_i) \quad (99)$$

We get the points and weights from the theory of Gaussian quadrature.

We now start describing the HEG method for calculating the potential energy matrix elements. In the end of the procedure we describe how we can use these matrix elements to compute eigenvalues and eigenfunctions of the full Hamiltonian. We start by constructing the $N \times N$ matrix representation \mathbf{X}_N of the \hat{x} operator with the help of the N basis functions. This matrix has the following elements

$$X_{mn} = \int_a^b \phi_m(x) x \phi_n(x) dx = \int_a^b w(x) p_m(x) x p_n(x) dx \quad (100)$$

The matrix \mathbf{X}_N is tridiagonal, which comes from the form of the three-term recursion relation fulfilled by orthogonal polynomials. After we have constructed \mathbf{X}_N , we diagonalize it by the following unitary transformation

$$\mathbf{U}_N^\dagger \mathbf{X}_N \mathbf{U}_N = \mathbf{x} \quad (101)$$

where $\mathbf{x}_{ij} = x_i \delta_{ij}$. We continue by computing $V(\mathbf{x})$. Because \mathbf{x} is diagonal, we have that $(V(\mathbf{x}))_{ij} = V(x_i) \delta_{ij}$. $V(\mathbf{x})$ is after this transformed to the basis of orthogonal polynomials, to express it formal

$$\mathbf{V}_N^{HEG} = \mathbf{U}_N V(\mathbf{x}) \mathbf{U}_N^\dagger \quad (102)$$

By adding the kinetic and potential parts the approximate Hamiltonian matrix is constructed

$$\mathbf{H}_N^{HEG} \equiv \mathbf{T}_N + \mathbf{V}_N^{HEG} \quad (103)$$

and finally we diagonalize the matrix \mathbf{H}_N^{HEG} to solve the time-independent Schrödinger equation or to propagate the time-dependent Schrödinger equation. We will now look at the expression $\mathbf{V}_N^{HEG} = \mathbf{U}_N V(\mathbf{x}) \mathbf{U}_N^\dagger$ from two different angles. First if we multiply out the matrices and use $\Phi_{in} = \sqrt{W_i} P_n(x_i)$. We get

$$(\mathbf{V}_N^{HEG})_{mn} = \sum_{i=1}^n \mathbf{U}_{mi} V(\mathbf{x}_{ii}) (\mathbf{U}^\dagger)_{in} = \sum_{i=1}^n W_i p_m(x_i) V(x_i) p_n(x_i) \quad (104)$$

This expression is the same as the one we get from an N -point Gaussian quadrature approximation to the integral $(\mathbf{V}_N(\hat{x}))_{mn}$ under the condition that the Gaussian quadrature points are identified with (x_i) and that the Gaussian weights are identified with (W_i) .

Second consider the following result

$$\mathbf{V}_N^{HEG} = \mathbf{U}_N V(\mathbf{x}) \mathbf{U}_N^\dagger = V(\mathbf{X}_N) \quad (105)$$

so the important approximation in the HEG method is the following substitution $\mathbf{V}_N \rightarrow V(\mathbf{X}_N)$

The matrices with subscript N are defined in the basis of orthogonal functions. But the approximation in the HEG method can be expressed in a basis-independent way. To the operator $\hat{x}_N = P_N \hat{x} P_N$ corresponds the matrix \mathbf{X}_N . So the approximation in the HEG method can be expressed as the substitution

$$P_N V(\hat{x}) P_N = V_N(\hat{x}) \rightarrow V(\hat{x}_N) = V(P_N \hat{x} P_N) \quad (106)$$

So we have a basis-independent representation.

4.5.2 The DVR method

The DVR method is a pseudospectral method for calculating matrix elements of the Hamiltonian. One important thing with the DVR method is that the pseudospectral basis is connected to the spectral basis through an orthogonal collocation matrix which is based on Gaussian quadrature points and weights. We start with the Hamiltonian $H = T(\hat{p}) + V(\hat{x})$. We are looking for an orthogonal projection onto Ξ_N . We express the projector in terms of the pseudospectral

basis, $P_N = \sum_{i=1}^N |\theta_i\rangle\langle\theta_i|$. By looking at $H_N = P_N T(\hat{p}) P_N + P_N V(\hat{x}) P_N$ in the pseudospectral basis we have that the matrix elements is of the following form

$$\langle\theta_i | T(\hat{p}) | \theta_j\rangle \quad (107)$$

and

$$\langle\theta_i | V(\hat{x}) | \theta_j\rangle \quad (108)$$

These basis functions (θ_i) are localized and fulfill the following orthonormality relation $\langle\theta_i | \theta_j\rangle = \delta_{ij}$. So it's reasonable to do the following substitution

$$V_{ij} = \langle\theta_i | V(\hat{x}) | \theta_j\rangle \rightarrow V(x_i)\delta_{ij} \quad (109)$$

This substitution is the important step when it comes to pseudospectral methods. The important approximation in the DVR method is the fact that the potential energy matrix \mathbf{V}^{DVR} is diagonal. As a consequence of this we only need the value of the potential at the DVR points. Because of this we don't have to perform the expensive and in some cases difficult numerical integration over the basis functions. For the DVR method this substitution represents an approximation which is identical to the Gaussian quadrature approximation which was used in the HEG method. We will come back to this later. But we can see this in because in the DVR method we have that the orthogonal collocation matrix is based on Gaussian quadrature points and weights. This gives that the pseudospectral basis functions fulfill the following equation $\hat{x}_N |\theta_i\rangle = x_i |\theta_i\rangle$. All this together with that the important approximation in the HEG method can be expressed as $P_N V(\hat{x}) P_N \rightarrow V(\hat{x}_N)$ and by using $P_N = \sum_{i=1}^N |\theta_i\rangle\langle\theta_i|$ the DVR pseudospectral matrix elements become

$$\begin{aligned} V(\hat{x}_N)_{ij} &= \sum_{k,l=1}^N \langle\theta_i | V(|\theta_k\rangle\langle\theta_k | \hat{x} | \theta_l\rangle\langle\theta_l |) | \theta_j\rangle \\ &= \sum_{k=1}^N \langle\theta_i | V(|\theta_k\rangle x_k \langle\theta_k |) | \theta_j\rangle \\ &= \sum_{k=1}^N \langle\theta_i | \theta_k\rangle V(x_k) \langle\theta_k | \theta_j\rangle = V(x_i)\delta_{ij} \end{aligned} \quad (110)$$

We consider now how to calculate the kinetic energy matrix in a pseudospectral basis. We start with calculating the second derivative matrix elements T_{ij} between two localized basis functions. These basis functions are associated with the grid points i and j .

$$\begin{aligned} (\mathbf{T}^\theta)_{ij} &= \langle\theta_i | T | \theta_j\rangle \\ &= \sum_{n,m=1}^N \langle\theta_i | \phi_n\rangle \langle\phi_n | T | \phi_m\rangle \langle\phi_m | \theta_j\rangle \\ &= \sum_{n,m=1}^N \Phi_{in}(\mathbf{T}^\phi)_{nm} \Phi_{mj}^\dagger = (\mathbf{\Phi} \mathbf{T}^\phi \mathbf{\Phi}^\dagger)_{ij} \end{aligned} \quad (111)$$

where \mathbf{T}^θ and \mathbf{T}^ϕ respectively are the kinetic energy matrix in pseudospectral basis and spectral basis and $\mathbf{\Phi}$ are the transformation between the spectral

and pseudospectral basis. We can also express these second derivative matrix elements in the following way

$$(\mathbf{T}^\theta)_{ij} = \sum_{n=1}^N \langle \theta_i | \phi_n \rangle \langle \phi_n | T | \theta_j \rangle \approx -\frac{\hbar^2}{2m} \sum_{n=1}^N \phi_n(x_i) \frac{\partial^2 \phi_n}{\partial x^2} |_{x_j} \quad (112)$$

This gives how the second derivative matrix between two pseudospectral functions can be calculated approximately.

We now take the DVR method up for discussion. It differs from the HEG method in that the unitary transformation is taken on the kinetic energy matrix, not on the potential energy matrix. We now start to describe the DVR method. The matrix representation \mathbf{X}_N of \hat{x} is constructed in a truncated basis consisting of N orthogonal polynomials. The constructed matrix \mathbf{X}_N is tridiagonal. This matrix is diagonalized by a unitary transformation

$$\mathbf{U}^\dagger \mathbf{X}_N \mathbf{U} = \mathbf{x} \quad (113)$$

where $(\mathbf{x})_{ij} = x_i \delta_{ij}$. We continue by computing $V(\mathbf{x})$. Because \mathbf{x} is diagonal, we have that $(V(\mathbf{x}))_{ij} = V(x_i) \delta_{ij}$. The calculation of the kinetic energy matrix takes place in the basis of orthogonal polynomials. We denote the matrix as \mathbf{T}_N^ϕ . The matrix elements are usually known analytically and the matrix is diagonal or tridiagonal. If we want to express in the pseudospectral basis the Hamiltonian $\mathbf{H}_N = \mathbf{T}_N + \mathbf{V}_N$ completely. The transformation \mathbf{U} which was used to transform the matrix \mathbf{V}_N to the pseudospectral basis must be used to transform \mathbf{T}_N^ϕ :

$$\mathbf{T}_{ij}^{DVR} = (\mathbf{U}^\dagger \mathbf{T}^\phi \mathbf{U})_{ij} \quad (114)$$

By adding the kinetic and potential energies, the DVR Hamiltonian is constructed

$$\mathbf{H}_N^{DVR} = \mathbf{T}_N^{DVR} + \mathbf{V}_N^{DVR} \quad (115)$$

and finally the DVR Hamiltonian \mathbf{H}_N^{DVR} is diagonalized.

The orthogonal projection of the Hamiltonian onto Ξ_N is constructed in the HEG method by using a spectral basis (ϕ_i) and in the DVR method by using a pseudospectral basis (θ_i) . In the DVR method the Hamiltonian is constructed in the pseudospectral basis (θ_i) . The two bases are connected by an unitary transformation

$$\mathbf{U} \mathbf{H}_N^{DVR} \mathbf{U}^\dagger = \mathbf{H}_N^{HEG} \quad (116)$$

From this follows that they have identical eigenvalues and if we use them to propagate an initial wavefunction. The dynamics will be the same in both cases.

We have then that the DVR method and HEG method have the same approximation of N -point Gaussian quadrature integration, since the HEG method can be basis-independent. The approximation is independent of the basis and the numerical results should be identical whether calculated in a spectral basis or in a pseudospectral basis. So the pseudospectral matrix elements of the potential in the DVR method can be calculated as

$$\begin{aligned} \langle \theta_i | V(\hat{x}) | \theta_j \rangle &= \int \theta_i(x) V(x) \theta_j(x) dx \\ &= \sum_{k=1}^N W_k \theta_i(x_k) \theta_j(x_k) = V(x_i) \delta_{ij} \end{aligned} \quad (117)$$

given that $\theta_i(x)V(x)\theta_j(x) = w(x)f(x)$ where $f(x)$ is a polynomial of degree $2N - 1$ or less.

4.6 The Fourier method

The Fourier method is a pseudospectral method where the points are evenly spaced on a grid. The value of the potential at the grid points gives the potential energy matrix. This matrix is diagonal. The Fourier method has two implementations: First the Fourier grid Hamiltonian (FGH) method and second the fast Fourier transform (FFT) method.

But before looking at these two methods, some preliminaries will be discussed. We start with the orthogonal basis functions in the Fourier method. These basis functions are of the form $\phi_k(x)\alpha e^{ikx}$. We have also that the projector is dependent on the choice of the range of x and the range of k , respectively. We will describe two cases, a continuous basis in k and a discrete basis in k . We start with the continuous k-basis.

The Hilbert space is restricted to $-K \leq k \leq K$. In the case the coordinate space range is infinite, we have that the k -normalized basis functions are

$$\phi_k(x) = \frac{e^{ikx}}{\sqrt{2\pi}} \quad (118)$$

where $-K \leq k \leq K$ and $-\infty < x < \infty$

The basis set which corresponds to the continuous values of k defines the following projection operator

$$P_{\Gamma}(\hat{p}) = \int_{-K}^K |\phi_k\rangle\langle\phi_k| dk \quad (119)$$

We now consider the case with an discrete k-basis. We start by making the assumption that the Hilbert space has finite support. To be more explicit the Hilbert space spans a finite range of the coordinate space, $0 \leq x \leq L$. We define a projection operator which is associated with the range

$$P_{\Gamma}(\hat{x}) = \int_0^L |x\rangle\langle x| dx \quad (120)$$

The following condition determines the normalized basis functions

$$\int_0^L \phi_k^*(x)\phi_{k'}(x)dx = \delta_{kk'} = \frac{1}{L} \int_0^L e^{-ikx}e^{ik'x}dx \quad (121)$$

This is only fulfilled for discrete values of k fulfilling the condition $k - k' = \frac{n2\pi}{L}$ or $\Delta k = \frac{2\pi}{L}$, where the difference between two neighboring basis functions in k is denoted as Δk . Thus, the normalized basis functions becomes

$$\phi_k(x) = \frac{e^{ikx}}{\sqrt{L}} \quad (122)$$

where $0 \leq x \leq L$ and $k = \kappa\Delta k$ where $-\infty < \kappa < \infty$

The restriction of k to discrete values corresponds to the following projection operator

$$P_{\square}(\hat{p}) = \sum_{\kappa=-\infty}^{\infty} |p_{\kappa}\rangle\langle p_{\kappa}| \quad (123)$$

where $p_\kappa = \hbar\kappa\Delta k$, since we have that $P_\square(\hat{x})$ and $P_\square(\hat{p})$ do not commute. The product of these operators is not hermitian and because of that the product is not a projector. But the product $P_\square(\hat{p})P_\square(\hat{p})$ is hermitian because both the projectors in the product are functions of \hat{p} . So we can use the projector

$$P = P_\square(\hat{p})P_\square(\hat{p}) \quad (124)$$

to combine the restriction of band-limit $-K \leq k \leq K$ and finite support on $0 \leq x \leq L$. We have used the assumption that $2K/\Delta k = KL/\pi = N$, N is an integer.

To the projection operator in (124) there corresponds a normalized basis (ϕ_κ) , so we have

$$P = P_\square(\hat{p})P_\square(\hat{p}) = \sum_{\kappa=1}^N |\phi_\kappa\rangle\langle\phi_\kappa| \quad (125)$$

where

$$\phi_\kappa(x) = \frac{e^{i\kappa\Delta kx}}{\sqrt{L}} = \frac{e^{i2\pi\kappa x/L}}{\sqrt{L}}, -\frac{N}{2} + 1 \leq \kappa \leq \frac{N}{2}, -\infty < x < \infty \quad (126)$$

We have two Fourier pseudospectral schemes corresponding to the continuous k -basis and the discrete k -basis. In each case the orthogonal collocation matrix is chosen so that the basis orthogonality relation becomes exact.

We start with the continuous k -basis.

$$\begin{aligned} \int_{-\infty}^{\infty} \phi_{k'}^*(x)\phi_k(x)dx &= \int_{-\infty}^{\infty} \frac{e^{i(k-k')x}}{2\pi} dx = \delta(k-k') \\ &= \sum_{j=-\infty}^{\infty} \phi_{k'}^*(x_j)\phi_k(x_j)\Delta x = \sum_{j=-\infty}^{\infty} \Phi_{k'}^*(x_j)\Phi_k(x_j) \end{aligned} \quad (127)$$

We make the following choice: $\Delta x = \frac{\pi}{K}$, $x_j = j\Delta x = \frac{j\pi}{K}$. The basis orthogonality relation is then fulfilled for

$$\Phi_k(x_j) = \frac{e^{ikx_j}}{\sqrt{2K}} \quad (128)$$

The grid orthogonality relation becomes

$$\int_{-K}^K \Phi_k(x_i)\Phi_k^*(x_j)dk = \int_{-K}^K \frac{e^{ik(x_i-x_j)}}{2K} dk = \delta_{ij} \quad (129)$$

In the discrete basis we choose the pseudospectral matrix so that the orthogonality relation becomes exact.

$$\int_0^L \phi_{\kappa'}^*(x)\phi_\kappa(x)dx = \delta_{\kappa\kappa'} = \sum_{j=1}^N \phi_{\kappa'}^*(x_j)\phi_\kappa(x_j)\Delta x = \sum_{j=1}^N \Phi_{\kappa'}^*(x_j)\Phi_\kappa(x_j) \quad (130)$$

We make the following choice: $\Delta x = \frac{L}{N}$ and $x_j = j\Delta x = \frac{jL}{N}$. The basis orthogonality relation is then fulfilled for

$$\Phi_\kappa(x_j) = \frac{e^{i2\pi\kappa j/N}}{\sqrt{N}} \quad (131)$$

The grid orthogonality relation becomes

$$\sum_{\kappa=-\frac{N}{2}+1}^{\frac{N}{2}} \Phi_{\kappa}(x_l) \Phi_{\kappa}^*(x_j) = \sum_{\kappa=-\frac{N}{2}+1}^{\frac{N}{2}} \frac{e^{i2\pi\kappa l/N}}{\sqrt{N}} \frac{e^{-i2\pi\kappa j/N}}{\sqrt{N}} = \delta_{lj} \quad (132)$$

in the case we have pseudospectral basis functions. The Fourier method have the following form in the continuous basis and the discrete basis respectively. The continuous one is

$$\int_{-K}^K \phi_{\kappa}(x) \phi_{\kappa}^*(x_j) dk = \theta_j(x) = \int_{-K}^K \frac{e^{ikx}}{\sqrt{2\pi}} \frac{e^{-ikx_j}}{\sqrt{2K}} dk \quad (133)$$

The discrete one is

$$\sum_{\kappa=-\frac{N}{2}+1}^{\frac{N}{2}} \phi_{\kappa}(x) \Phi_{\kappa}^*(x_j) = \theta_j(x) = \sum_{\kappa=-\frac{N}{2}+1}^{\frac{N}{2}} \frac{e^{i2\pi\kappa x/L}}{\sqrt{L}} \frac{e^{-i2\pi\kappa x_j/L}}{\sqrt{N}} \quad (134)$$

4.6.1 The FGH method

We consider now the FGH method which is a special case of the DVR method. The facts which provides the basis for the FGH method is that it is easier to construct the kinetic energy matrix \mathbf{T} in the momentum representation and the potential energy matrix \mathbf{V} in the coordinate representation. We have that Fourier transforms give us a method of transforming between these two representations. In the FGH method the transformation matrix is a Fourier matrix, which is a difference compared to the DVR method. In the FGH method the amplitude of the wavefunction on the grid points are used to generate the wavefunctions of the Hamiltonian operator or the eigenfunctions of the Hamiltonian operator. So the wavefunctions are not given by a linear combination of basis functions. With the Fourier grid Hamiltonian (FGH) method we evaluate the matrix elements of the Hamiltonian by using the Fourier pseudospectral scheme. We begin with the Hamiltonian operator expressed in the coordinate representation.

$$\begin{aligned} \langle x | H | x' \rangle &= \langle x | T(\hat{p}) + V(\hat{x}) | x' \rangle \\ &= \int_{-\infty}^{\infty} \langle x | k \rangle \frac{\hbar^2 k^2}{2m} \langle k | x' \rangle dk + V(x) \delta(x - x') \\ &= \frac{\hbar^2}{2m} \int_{-\infty}^{\infty} \frac{e^{ikx}}{\sqrt{2\pi}} k^2 \frac{e^{-ikx'}}{\sqrt{2\pi}} dk + V(x) \delta(x - x') \end{aligned} \quad (135)$$

In the Fourier pseudospectral scheme we discretize the coordinates x and x' at N points evenly spaced so that $x \rightarrow l\Delta x$ and $x' \rightarrow j\Delta x$. The Hamiltonian matrix is an $N \times N$ matrix and we say that H_{lj} corresponds to the position $l\Delta x$, $j\Delta x$. With the help of the DVR method we get the potential energy matrix elements. So the off-diagonal elements disappear and the diagonal elements are

$$\langle x_l | V(\hat{x}) | x_j \rangle \rightarrow V(x_j) \delta_{lj} \quad (136)$$

The kinetic energy matrix elements becomes

$$\begin{aligned}\langle x_l | T(\hat{p}) | x_j \rangle &= \int_{-\infty}^{\infty} \langle x_l | k \rangle \langle k | T(\hat{p}) | k \rangle \langle k | x_j \rangle dk \\ &= \frac{\hbar^2}{2m} \int_{-\infty}^{\infty} \frac{e^{ikl\Delta x}}{\sqrt{2\pi}} k^2 \frac{e^{-ikj\Delta x}}{\sqrt{2\pi}} dk\end{aligned}\quad (137)$$

The existence of the exponential factor and the integral over k can be seen as coming from a forward, followed by an inverse Fourier transform. Before continuing with the FGH method. We take up the procedure with discretization. Instead of a continuous range of coordinate values x we want to use a grid of discrete values x_l . So we use a uniform discrete grid of x values. There $x_l = l\Delta x$, where Δx denotes the uniform spacing between the different grid points. So for the wave function the normalization condition becomes

$$\int_{-\infty}^{\infty} \psi^*(x)\psi(x)dx = 1. \quad (138)$$

If we on a regular grid with N values of x discretize the integral in (138) we get

$$\sum_{i=1}^N \psi^*(x_i)\psi(x_i)\Delta x = 1. \quad (139)$$

The reciprocal grid size in momentum space is determined by the choice of the spacing in coordinate space and the grid size. The longest wavelength and as a consequence of that the smallest frequency occurring in the reciprocal momentum space $\Delta k = 2\pi/\lambda_{max}$ is determined by the length $N\Delta x$. This length is the part of coordinate space which is covered by the grid. The relation $\Delta k = 2\pi/N\Delta x$ then gives the grid spacing in momentum space. In the momentum space grid the middle point is chosen to be $k = 0$ and about this point the grid points are evenly distributed by the relation $2n = (N - 1)$, where we have defined an integer n and N is the number of grid points in the spatial grid. N is an odd integer. The case for N even is treated similarly. So the bras and kets of the discretized coordinate space give at the grid points the following value of the wave function

$$\langle x_i | \psi \rangle = \psi(x_i) = \psi_i. \quad (140)$$

The identity operator takes the following form $\hat{I}_x = \sum_{i=1}^N |x_i\rangle\Delta x\langle x_i|$ and the orthogonality condition becomes $\Delta x\langle x_i | x_j \rangle = \delta_{ij}$. So we continue now with the FGH method. First we truncate the range of integration to $[-K, K]$, where $K = \pi/\Delta x$ and the integral is discretized over k where the spacing Δk in k is $\frac{2\pi}{N\Delta x}$. This corresponds to the basis in the Fourier pseudospectral scheme. We infer the substitution $k = \kappa\Delta x$ and use the relation $\Delta k\Delta x = \frac{2\pi}{N}$ to get

$$\begin{aligned}\langle x_l | T(\hat{p}) | x_j \rangle &\approx \frac{\hbar^2}{2m} \sum_{\kappa=-\frac{N}{2}+1}^{\frac{N}{2}} \frac{e^{i2\pi\kappa l/N}}{\sqrt{2K}} (\kappa\Delta k)^2 \frac{e^{-i2\pi\kappa j/N}}{\sqrt{2K}} \Delta k \\ &= \frac{\hbar^2}{2m} \left(\frac{2K}{N}\right)^2 \sum_{\kappa=-\frac{N}{2}+1}^{\frac{N}{2}} \frac{e^{i2\pi\kappa l/N}}{\sqrt{N}} \kappa^2 \frac{e^{-i2\pi\kappa j/N}}{\sqrt{N}}\end{aligned}\quad (141)$$

So this equation has the form

$$\langle x_l | T(\hat{p}) | x_j \rangle = \sum_{\kappa=-\frac{N}{2}+1}^{\frac{N}{2}} \phi_{\kappa}(x_j) \frac{\hbar^2 \kappa^2}{2m} \phi_{\kappa}^*(x_l) = (\mathbf{U}^\dagger \mathbf{T} \mathbf{U})_{jl} \quad (142)$$

By adding the kinetic and potential energy we have

$$\mathbf{H}_{ij}^{FGH} = \mathbf{T}_{ij}^{FGH} + \mathbf{V}_{ij}^{FGH} \quad (143)$$

To summarize it the approximation of the FGH matrix is the following substitution

$$H \rightarrow H^{FGH} = P_{\sqcup}(\hat{p}) P_{\sqcap}(\hat{p}) H P_{\sqcap}(\hat{p}) P_{\sqcup}(\hat{p}) \quad (144)$$

or

$$H \rightarrow H^{FGH} = P_{\sqcap}(\hat{p}) H P_{\sqcap}(\hat{p}) \quad (145)$$

depending on the basis chosen.

4.6.2 The FFT method

We consider the FFT method. In this method the operation of $H\psi$ is calculated as described in the following way. The Hamiltonian operator is $H = T + V$. The method is to locally calculate the operators since the potential operator is local in coordinate space. Its operation is therefore a multiplication of $V(x_j)$ by $\psi(x_j)$. The local operation of the kinetic energy operator can be done in momentum space where it is a multiplication by the kinetic energy discrete spectrum: $T(k) = \frac{\hbar^2 k^2}{2m}$. The calculation of the kinetic energy operator starts with transforming ψ to momentum space by the help of a backward discrete Fourier transform (DFT) multiplying by $T(k)$ and after that transform back to coordinate space by the help of a forward discrete Fourier transform (DFT). The matrix-vector representation of $H\psi = (T + V)\psi$ is of the following form

$$\begin{aligned} & \frac{1}{N} \begin{pmatrix} 1 & 1 & 1 & \dots & 1 \\ 1 & w & w^2 & \dots & w^{N-1} \\ 1 & w^2 & w^4 & \dots & w^{2(N-1)} \\ \vdots & \vdots & \vdots & \ddots & \vdots \\ 1 & w^{N-1} & w^{2(N-1)} & \dots & w^{(N-1)^2} \end{pmatrix} \begin{pmatrix} T_0 & 0 & 0 & \dots & 0 \\ 0 & T_1 & 0 & \dots & 0 \\ 0 & 0 & T_2 & \dots & 0 \\ \vdots & \vdots & \vdots & \ddots & \vdots \\ 0 & 0 & 0 & \dots & T_{N-1} \end{pmatrix} \\ & \times \begin{pmatrix} 1 & 1 & 1 & \dots & 1 \\ 1 & w^{-1} & w^{-2} & \dots & w^{-(N-1)} \\ 1 & w^{-2} & w^{-4} & \dots & w^{-2(N-1)} \\ \vdots & \vdots & \vdots & \ddots & \vdots \\ 1 & w^{-(N-1)} & w^{-2(N-1)} & \dots & w^{-(N-1)^2} \end{pmatrix} \times \begin{pmatrix} \psi(x_0) \\ \psi(x_1) \\ \psi(x_2) \\ \vdots \\ \psi(x_{N-1}) \end{pmatrix} \\ & + \frac{1}{N} \begin{pmatrix} V(x_0) & 0 & 0 & \dots & 0 \\ 0 & V(x_1) & 0 & \dots & 0 \\ 0 & 0 & V(x_2) & \dots & 0 \\ \vdots & \vdots & \vdots & \ddots & \vdots \\ 0 & 0 & 0 & 0 & V(x_{N-1}) \end{pmatrix} \times \begin{pmatrix} \psi(x_0) \\ \psi(x_1) \\ \psi(x_2) \\ \vdots \\ \psi(x_{N-1}) \end{pmatrix} \end{aligned}$$

where

$$w = e^{2\pi i/N} \quad (146)$$

and

$$T_\kappa = \frac{\hbar^2(\kappa\Delta k)^2}{2m} \quad (147)$$

$\frac{1}{\sqrt{N}}$ are factored out from the orthogonal collocation matrices, where T_κ runs over $[-N/2+1, \dots, 0, \dots, N/2]$. But to be in accordance with the indexing of the FFT matrix the index of T is changed to run from $[0, \dots, N/2, -N/2+1, \dots, -1]$. We have now $H\psi(x, t_0)$. The advancement in time to get $\psi(x, t_1)$ can be done by various methods which will be discussed later. We repeat the procedure to get $\psi(x, t_2)$ and so on. This ends the description of the FFT method. The DFT methods discrete sampling in k -space is connected to periodic boundary conditions in x . That is to the basis which has been mentioned before

$$\phi_\kappa(x) = \frac{e^{i\kappa\Delta x}}{\sqrt{L}} = \frac{e^{i2\pi\kappa x/L}}{\sqrt{L}}, -\frac{N}{2} + 1 \leq \kappa \leq \frac{N}{2}, -\infty < x < \infty \quad (148)$$

We use an FFT algorithm where the number of multiplications is $\frac{1}{2}N \ln N$ to implement the DFT. In the case of a straightforward implementation of the DFT the number of multiplications is N^2 . When we compare the FFT method with the FGH method Tannor[17] mentions two main advantages with the FFT method. The first one is that the FFT algorithm rearranges the elements of the input vector so we don't need to construct and store any matrices. The second advantage is that when we use the FFT algorithm to implement the DFT, this method scales semilinearly with the number of points $N \ln N$. In the case of matrix multiplication the number of points is N^2 and in the case of matrix diagonalization is the number of points N^3 .

4.7 Phase space

A phase space interpretation can be given to every spectral and pseudospectral method. When a basis function is chosen, this choice of basis defines for a subspace of the Hilbert space a projection operator $P_N = \sum_{n=1}^N |\phi_n\rangle\langle\phi_n|$. The region of the phase space which is spanned by this basis can be represented by the Wigner transform of the projection operator

$$P_N^W(p, q) = \sum_{n=1}^N \frac{1}{2\pi\hbar} \int_{-\infty}^{\infty} \phi_n^*(q - \frac{s}{2}) \phi_n(q + \frac{s}{2}) e^{ips/\hbar} ds. \quad (149)$$

An interpretation of the projector P is expressed in terms of a region of phase space. This region is independent of the basis chosen that spans the truncated subspace. We now continue by studying the phase space in the Fourier method. First we have between the maximum wave number, K and the sampling number spacing Δx the following relation $K = \frac{\pi}{\Delta x}$. We infer the following $k_{range} = k_{max} - k_{min} = 2K$ which gives $k_{range} = \frac{2\pi}{\Delta x}$. In a similar way we get $x_{range} = \frac{2\pi}{\Delta k}$. So we have a correspondence between the grid spacing in coordinate space and the grid range in momentum space. There is also a correspondence between the grid range in coordinate space and grid spacing in momentum space. The product of the range of the grid in momentum and coordinate gives the volume in phase space which is covered by the Fourier representation. Since we have

the relations $x_{range} = L, \Delta x = \frac{L}{N}$ and $p_{range} = \hbar k_{range}$, where N is the number of grid points, we have that the phase space volume becomes $\frac{L\hbar}{\Delta x} = Nh$. We can give this result the following interpretation: The number of grid points is proportional to the volume in phase space and the phase space volume per grid point is Planck's constant. So we can use the phase space representation to analyze the Fourier method efficiency.

5 Time propagation

When we consider numerical solutions for the time-dependent Schrödinger equation we must make some approximations about the development of time of the Hamiltonian. We have up to this point only discussed numerical methods for executing the operation $H\psi$ on a grid of points. We now consider the case of numerical implementation of the following expression $e^{-iHt/\hbar}\psi$. We will now consider different methods for this implementation.

5.1 The split operator method

In the split operator method we use the ease of treating operators in their diagonal representations. We start describing the propagator over the time interval $[0, t]$ as a product of propagators over time intervals Δt where $N\Delta t = t$. So we have

$$U(0, t) = e^{-iHt/\hbar} = e^{-iH\Delta t/\hbar} \dots e^{-iH\Delta t/\hbar} \quad (150)$$

where $e^{-iH\Delta t/\hbar}$ is multiplied N times.

The idea is to approximate each of these time propagators over Δt as a product of a kinetic and a potential factor.

$$e^{-iH\Delta t/\hbar} = e^{-i(\hat{p}^2/2m + V(\hat{x}))\Delta t/\hbar} \approx e^{-i(T\Delta t/\hbar)} e^{-i(V\Delta t/\hbar)} + O(\Delta t^2) \quad (151)$$

where $T = \hat{p}^2/2m$.

T is diagonal in momentum space and V is diagonal in coordinate space. If T and V commuted then the product would be exact. So the error should be proportional to the commutator $[T, V]$. The truncated error is determined by the next higher commutator between the potential and the kinetic energy and will vary with the value of these terms.

By the multiplication of $e^{-iV(\hat{x})\Delta t/\hbar}$ with $\psi(x)$ we calculate the operation

$$e^{-iV(\hat{x})\Delta t/\hbar}\psi$$

and in a similar way the operation

$$e^{-iT(\hat{p})\Delta t/\hbar}\psi = e^{-i\hat{p}^2\Delta t/2m\hbar}\psi$$

is calculated by $Z e^{-iT_{pp'}\Delta t/2m\hbar} Z^\dagger \psi(x)$, where we have that Z^\dagger is the transformation between the momentum and coordinate representation and $T_{pp'}$ is the diagonal representations of the kinetic energy in momentum space. We now take up the question about the applications of the split operator method. In most cases it is implemented in the Fourier basis. We have that in the Fourier basis Z^\dagger is a discrete Fourier transform (DFT) with matrix elements $Z_{lj}^\dagger = \frac{1}{\sqrt{N}} e^{ip_l x_j/\hbar}$. These elements can be calculated by the help of an FFT.

The FFT algorithm provides an accurate unitary transformation between two finite representations on grids with N points. The split operator method has the following properties. It is unitary and preserves norm. The split operator method is unconditionally stable. It is used if the Hamiltonian is written as a sum of operators that depends on coordinates or momenta, respectively. But in the case we have operators where coordinates and momenta is entangled, we can not use the method; To take an example operators of the form $e^{i\hat{p}\hat{x}}$. The method has been used to treat bound eigenstate determination and wave packet scattering time-dependent Hamiltonian functions.

5.2 Polynomial methods

In the polynomial methods the propagator is represented as

$$e^{-iHt/\hbar}\psi = \sum_n a_n P_n(H)\psi \quad (152)$$

where $P_n(H)$ is a polynomial of the Hamiltonian operator, whose operation on ψ can be evaluated by iteration of H on ψ . Since we know for instance how to calculate $H\psi$ for pseudospectral methods, we can calculate $H(H\psi)$ and finally $H^n\psi$ for any n by iteration. So $P_n(H)\psi$ can be calculated for any polynomial of H . When we have chosen a polynomial sequence, the coefficients a_n are uniquely determined. We can divide the polynomial methods into one category that chooses the polynomial in advance (uniform methods) and one category which does not choose the polynomial in advance (non-uniform methods). As an example of the first type we can take the Chebyshev method and as an example of the second type we can take the short iterative Lanczos method.

5.2.1 The Chebyshev method

Consider a scalar function $f(x)$, where $x \in [-1, 1]$ and $f(x) = \sum a_n P_n(x)$. If this is the case the Chebyshev polynomial approximation is optimal, because the maximum error in the approximation is minimal when compared to every possible polynomial approximation when it comes to practical use. We will now look at the expansion of the propagator in terms of Chebyshev polynomials and consider how the exponential functions are represented in the terms of the Chebyshev polynomials. For exponential functions the expansion has the following form

$$e^{-i\alpha x} = \sum a_n(\alpha) \Phi_n(-ix) \quad (153)$$

where

$$a_n(\alpha) = \int_{-i}^i \frac{e^{i\alpha x} \Phi_n(x)}{\sqrt{1-x^2}} dx = 2J_n(\alpha) \quad (154)$$

and

$$a_0(\alpha) = J_0(\alpha) \quad (155)$$

where the $J_n(\alpha)$ are Bessel functions of the first kind (see Andersson and Böiers[2]). Time reversal symmetry is built into the expansion coefficients.

The Chebyshev recurrence relation is

$$\Phi_{n+1} = -2ix\Phi_n + \Phi_{n-1} \quad (156)$$

Before we start implementing the expansion in (153) for the propagator, we have to map the argument $-iHt/\hbar$ onto the domain $[-i, i]$. So we have

$$H_{norm} = 2 \frac{H - I(\Delta E_{grid}/2 + E_{min})}{\Delta E_{grid}} \quad (157)$$

where we infer $\Delta E_{grid} = E_{max} - E_{min}$ which is the range of energy supported by the grid. I is the $N \times N$ identity matrix.

We also infer that $E_{max} = V_{max} + T_{max}$ which is the maximum energy supported by the grid and $E_{min} = V_{min}$ is the minimum energy which is supported by the grid. Finally we infer $T_{max} = \hbar^2 k_{range}^2 / 2m$ which is the maximum kinetic energy supported by the grid where $k_{range} = \pi / \Delta x$. When we have this mapping, the wavefunction becomes

$$\psi(t) \approx e^{-i(E_{min}t/\hbar + \alpha)} \sum_n a_n(\alpha) \Phi_n(-iH_{norm}) \psi(0) \quad (158)$$

where Φ_n are the complex Chebyshev polynomials and $\alpha = \frac{\Delta E_{grid} t}{2\hbar}$. The following recurrence relation generates the polynomials.

$$\phi_{n+1} = -2iH_{norm}\phi_n + \phi_{n-1} \quad (159)$$

where $\phi_n = \Phi_n(-iH_{norm})\psi(0)$. The recurrence starts with

$$\phi_0 = \psi(0) \quad (160)$$

and

$$\phi_1 = -iH_{norm}\psi(0) \quad (161)$$

We consider the expansion coefficients as a function of n . One thing which is seen is that when n is larger than α , we have that the Bessel functions $J_n(\alpha)$ decay exponentially. This means that when it comes to practical implementation, we can choose the maximum order N in such a way that the accuracy of the computer dominates the accuracy. We have that the Chebyshev propagator in an effective way in a single time step does the propagation. We can not automatically obtain the intermediate time results. But because we have that all the time dependence is in the Bessel function coefficients and none of the spatial dependences, we know when the calculation of the Chebyshev polynomials is finished. The information at the intermediate times can be given at a low cost. One important thing with the Chebyshev propagation method is the fact that the error is uniformly distributed over the total range of eigenvalues. The Chebyshev method is not unitary but its accuracy gives that the deviation from unitary can be employed as a test of accuracy.

5.2.2 The Lanczos method

We begin by defining the Krylov space. The Krylov space is a subspace of the full Hilbert space. We obtain the Krylov space if we on an initial state act with a linear operator, say N times. Let us consider the following example.

We have that the linear operator is the Hamiltonian. We denote it as H and it is hermitian. The vectors $u_j = H^j \psi(0)$ then span the Krylov space. By the Lanczos method can we construct a matrix representation of the Hamiltonian.

This matrix representation can be expressed in a basis which is spanned by the Krylov space $K_N = (\psi(0), H\psi(0), H^2\psi(0), \dots, H^{N-1}\psi(0))$. We diagonalize the Hamiltonian matrix and we use the diagonal representation to propagate the initial state inside the Krylov space. Because the operator H is used to construct the Krylov space, the Krylov space is constructed to include that part of the Hilbert space in which the wavefunction is in the nearest moments.

We have that the functions which defines the Krylov space, $u_j = H^j\psi(0)$ are in most cases not orthogonal. For practical use it is for most cases more convenient to use orthogonal functions. In the Lanczos method, when a new Krylov vector is constructed, it is also orthogonal to all the previous Krylov vectors. To describe the procedure, we have that the first basis function q_0 is the initial state $|\phi_0\rangle = \psi(0)$.

We start our construction by letting H act on $|\phi_0\rangle$ and we get

$$H|\phi_0\rangle = \alpha_0|\phi_0\rangle + |\Phi_1\rangle \quad (162)$$

where

$$\langle\phi_0|\Phi_1\rangle = 0 \quad (163)$$

and

$$\alpha_0 = \langle\phi_0|H|\phi_0\rangle \quad (164)$$

We continue by expressing the new state in the following way

$$|\Phi_1\rangle = (1 - P_0)H|\phi_0\rangle = H|\phi_0\rangle - \alpha_0|\phi_0\rangle \quad (165)$$

where $P_0 = |\phi_0\rangle\langle\phi_0|$. We continue by normalizing $|\Phi_1\rangle$

$$|\phi_1\rangle = \frac{1}{\beta_1}|\Phi_1\rangle, \beta_1^2 = \langle\Phi_1|\Phi_1\rangle \quad (166)$$

Next we look at to the matrix element

$$\langle\phi_1|H|\phi_0\rangle = \langle\phi_1|\Phi_1\rangle + \langle\phi_1|P_0H|\phi_0\rangle = \beta_1 \quad (167)$$

So the next step is to apply H on $|\phi_1\rangle$. The new state will have some overlap with $|\phi_0\rangle$ and $|\phi_1\rangle$. We redefine the new state $|\Phi_2\rangle$ and by introducing the projection operator $P_1 = |\phi_1\rangle\langle\phi_1|$ in the following way.

$$|\Phi_2\rangle = (1 - P_1)(1 - P_0)H|\phi_1\rangle = (1 - P_1 - P_0)H|\phi_1\rangle = H|\phi_1\rangle - \alpha_1|\phi_1\rangle - \beta_1|\phi_0\rangle \quad (168)$$

We have $\alpha_1 = \langle\phi_1|H|\phi_1\rangle$. The normalized version of $|\Phi_2\rangle$ becomes in the same way as before

$$|\phi_2\rangle = \frac{1}{\beta_2}|\Phi_2\rangle, \beta_2^2 = \langle\Phi_2|\Phi_2\rangle \quad (169)$$

We have that $\langle\phi_1|H|\phi_2\rangle = \beta_2$ and $\langle\phi_0|H|\phi_2\rangle = 0$.

So the common pattern looks like

1. $|\Phi_{j+1}\rangle = H|\phi_j\rangle - \alpha_j|\phi_j\rangle - \beta_j|\phi_{j-1}\rangle$
2. $\alpha_j = \langle\phi_j|H|\phi_j\rangle$

$$3. |\phi_j\rangle = \frac{1}{\beta_j} |\Phi_j\rangle, \beta_j^2 = \langle \Phi_j | \Phi_j \rangle$$

So for the general expression we have the following form

$$H |\phi_j\rangle = \beta_{j+1} |\phi_{j+1}\rangle + \alpha_j |\phi_j\rangle + \beta_j |\phi_{j-1}\rangle \quad (170)$$

where we have that the coefficients are $\alpha_j = \langle \phi_j | H | \phi_j \rangle$ and $\beta_j = \langle \phi_j | H | \phi_{j-1} \rangle$

Below is the matrix elements of the Hamiltonian in the Lanczos basis. This matrix is as seen tridiagonal.

$$H_N = \begin{pmatrix} \alpha_0 & \beta_1 & 0 & \dots & \dots & \dots & 0 \\ \beta_1 & \alpha_1 & \beta_2 & 0 & \dots & \dots & 0 \\ 0 & \beta_2 & \alpha_2 & \beta_3 & 0 & \dots & 0 \\ \vdots & \vdots & \ddots & \ddots & \vdots & \vdots & 0 \\ 0 & \dots & \dots & \dots & \beta_{N-2} & \alpha_{N-2} & \beta_{N-1} \\ 0 & \dots & \dots & \dots & \dots & \beta_{N-1} & \alpha_{N-1} \end{pmatrix}$$

We diagonalize H_N and get

$$Z^\dagger H_N Z = D_N \quad (171)$$

where D_N is a diagonal matrix consisting of the eigenvalues of H_N . The transformation matrix Z is used to express the propagator. It becomes

$$U(\Delta t) = e^{-iH_N \Delta t / \hbar} = e^{-iZ D_N Z^\dagger \Delta t / \hbar} = Z e^{-iD_N \Delta t / \hbar} Z^\dagger \quad (172)$$

So the propagated wavefunction is of the following form

$$\psi(\Delta t) = Z e^{-iD_N \Delta t / \hbar} Z^\dagger \psi(0) \quad (173)$$

The eigenvalues and corresponding eigenvectors of H_N can be calculated by an accuracy of $O(N^2)$.

We have mentioned before that the Krylov space which is spanned by $u_j = H^j \psi(0)$ spans the subspace of the Hilbert space where $\psi(0)$ in short times will evolve in. This comes from the fact that it is also the subspace which is spanned by the Taylor series expansion of the propagator valid at short times. The size of the Krylov space is important for how long time the evolving wave packet is confined inside the Krylov space. To put it in other words. The size of the generated Krylov space gives for how long time we will be able to study the packet dynamics. One can prove that for a finite Hilbert space (a N -level system) that a Krylov space of size N generates within numerical error, the exact dynamics. When it comes to practical use there is a choice between two different approaches. First generating a large Krylov space and use the generated Krylov space for a long time stop propagation and second generating a small Krylov space but use the Krylov space for short time steps where the Krylov space is frequently updated generating a new Krylov space by the help of the current initial state. This second method is called the short iterative Lanczos method.

We can summarize the Lanczos method in a more general way. We have this Krylov space $K_N = (\psi(0), H\psi(0), H^2\psi(0), \dots, H^{N-1}\psi(0)) = (q_1, q_2, \dots, q_N)$

where the vectors q_j are orthonormal. We express it in matrix form. Let Y_N be the Krylov matrix of the following form

$$Y_N = [\psi(0) \mid H\psi(0) \mid \dots \mid H^{N-1}\psi(0)] \quad (174)$$

Then Y_N has a reduced QR factorization (see Bau and Trefethen [3])

$$Y_N = Q_N R_N \quad (175)$$

where Q_N is

$$Q_N = [q_1 \mid q_2 \mid \dots \mid q_N] \quad (176)$$

So the matrices Q_j of vectors q_j which are generated by the Lanczos method are reduced QR factors of the Krylov matrix

$$Y_j = Q_j R_j \quad (177)$$

The corresponding projections are the tridiagonal matrices T_j

$$T_j = Q_j^\dagger H Q_j \quad (178)$$

and by the following formula we have a relation between the successive iterates

$$H Q_j = Q_{j+1} \tilde{T}_j \quad (179)$$

which we can express as a three-term recurrence at step j .

$$H q_j = \beta_{j-1} q_{j-1} + \alpha_j q_j + \beta_j q_{j+1} \quad (180)$$

as long as Y_j is of full rank. We have that the characteristic polynomial of T_j is the unique polynomial $p^j \in P^j$ that fulfills

$$\| p^j(H)q \| = \text{minimum} \quad (181)$$

The usefulness of the Lanczos algorithm consists of that the multiplication by H is the only large scale linear operation. To take an example Lanczos iteration is used to compute eigenvalues of large symmetric matrices.

5.3 The second-order differencing method

The simplest method for time propagation is to expand

$$e^{-iH\Delta t/\hbar} = 1 - iH\Delta t/\hbar + \dots \quad (182)$$

in a Taylor series. But a numerical algorithm which is based on this expansion is not stable. We have that this instability comes from the fact that the time reversal symmetry of the Schrödinger equation is not conserved with this method. But with the help of a symmetric modification of the expansion can we achieve stability. So we can formulate the method by using second-order differencing (SOD) to make an approximation of the time derivative in the Schrödinger equation. Another formulation is to use the following relation

$$\psi(t + \Delta t) - \psi(t - \Delta t) = (e^{-iH\Delta t/\hbar} - e^{iH\Delta t/\hbar})\psi(t) \quad (183)$$

If we expand the exponential functions in (183) in a Taylor series. We get the following second-order propagation scheme.

$$\psi(t + \Delta t) \approx \psi(t - \Delta t) - 2i\Delta t H \psi(t) / \hbar \quad (184)$$

so we have in Dirac notation the following expression for the SOD method

$$|\phi, t + \Delta t\rangle - |\phi, t - \Delta t\rangle = -2iH\Delta t/\hbar |\phi, t\rangle + O((H\Delta t)^3). \quad (185)$$

In the SOD method or MSD2 method to start the propagation we need two initial conditions. The initialization scheme and the propagation should have equal accuracy. To describe how the method is used, let us begin with a first-order scheme for half a time step. Continue by using the SOD method to propagate another half step. We have now two initial conditions $\psi(t)$ and $\psi(t + \Delta t)$. Another method which is more symmetric when it comes to time reversal is to first propagate half a step backward to get $\psi(t - \Delta t)$ and after that half a step forward to get $\psi(t + \Delta t)$. The propagation continues and we can get the intermediate results by the following approximation

$$\psi(t) \approx \frac{1}{2}[(\psi(t - \Delta t/2) + \psi(t + \Delta t/2)) + \frac{i}{\hbar}\Delta t/2(H\psi(t + \Delta t/2) - H\psi(t - \Delta t/2))] \quad (186)$$

This approximation is accurate up to second order. If it is the case that the Hamiltonian operator is hermitian, then we have that the SOD propagation scheme is stable and it preserves norm and energy. We have that the time reversal symmetry is built into the system. We now mention something about the error. First we have that the error in the propagation is accumulated in phase. Second we have that if we propagate N times the error is accumulated N times. Now the third and final comment. If we look at the scaling of the numerical effort for a fixed time, we have that the error scales as $O(1/N^2)$, where N is the number of times we call the Hamiltonian operator. In the case of a constant error we have that the numerical effort scales as $O(t^{3/2})$.

5.4 The Crank-Nicholson method

This method is recommended for solving the time-dependent Schrödinger equation using finite difference methods. This method is an implicit method. The Crank-Nicholson method is a special case of an implicit Adams method. Let us start by considering the equation

$$\frac{du(t)}{dt} = f(t, u(t)) \quad (187)$$

where

$$u(t_0) = u_0 \quad (188)$$

If u solves this equation we get

$$u(t_{n+1}) - u(t_n) = \int_{t_n}^{t_{n+1}} f(t, u(t)) dt \quad (189)$$

$f(t, u(t))$ is then replaced by an interpolation polynomial P having the value $F_j = f(t_j, U_j)$ at t_j for $n - q + 1 \leq j \leq n + 1$. Since we have finite differences

on a uniform grid (see Schatzman[14]), we get

$$P(t_n + hs) = \sum_{i=0}^q (-1)^i \binom{-s+1}{i} (\nabla^i F)_{n+1}. \quad (190)$$

If we define

$$\gamma_i^* = (-1)^i \int_0^1 \binom{-s+1}{i} ds \quad (191)$$

the family of implicit Adams methods is then given by

$$U_{n+1} = U_n + h \sum_{i=0}^q \gamma_i^* (\nabla^i F)_{n+1}. \quad (192)$$

The recurrence relation for the γ_i^* is

$$\begin{aligned} \gamma_0^* &= 1 \\ \frac{\gamma_0^*}{2} + \gamma_1^* &= 0 \\ &\vdots \\ \frac{\gamma_0^*}{n+1} + \dots + \frac{\gamma_{n-1}^*}{2} + \gamma_n^* &= 0 \end{aligned}$$

The case $q = 2$ corresponds to the Crank-Nicholson method. We consider now the time-dependent Schrödinger equation. The Hamilton operator is discretized at L positions. These positions are equidistant with a separation of length Δx on the real axis. By ψ_j we denote the value of ψ at the point $x_j = j\Delta x$, $j = 1, \dots, L$. We call the discretized Hamiltonian H_D and the Schrödinger equation can be expressed as

$$i\hbar \frac{d\psi_j(t)}{dt} = H_D \psi_j(t). \quad (193)$$

By using time intervals Δt we discretize time. The upper index to the wave function ψ is used to denote time. We have that we can approximate the time derivative of ψ_j^n at this particular time step with the expression $(\psi_j^{n+1} - \psi_j^n)/\Delta t$ where the error is of the order Δt , so we get

$$\psi_j^{n+1} = (1 - i\Delta t H_D/\hbar) \psi_j^n. \quad (194)$$

By the help of the expression of the implicit form can we derive the Crank-Nicholson method. But a much easier way is the following heuristic derivation. $|t + \delta t\rangle = e^{-iH\Delta t/\hbar} |t\rangle = e^{-iH\Delta t/(2\hbar)} e^{-iH\Delta t/(2\hbar)} |t\rangle \Rightarrow e^{iH\Delta t/(2\hbar)} |t + \Delta t\rangle = e^{-iH\Delta t/(2\hbar)} |t\rangle$

By using Taylor expansion on the exponential we get

$$(1 + \frac{iH\Delta t}{2\hbar}) |t + \Delta t\rangle = (1 - \frac{iH\Delta t}{2\hbar}) |t\rangle$$

So we get the following expression for the Crank-Nicholson method

$$|t + \Delta t\rangle = \frac{(1 - \frac{iH\Delta t}{2\hbar})}{(1 + \frac{iH\Delta t}{2\hbar})} |t\rangle$$

It is stable and unitary and correct up to second order in Δt . As mentioned before this is an implicit method, so a matrix inversion must be done at every time step.

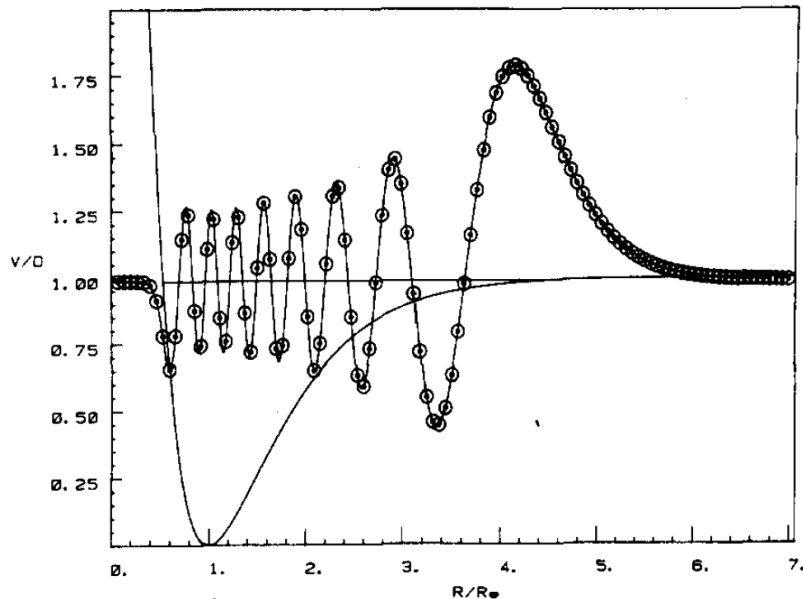


Figure 1: Comparison of analytic (solid line) and numerically computed (dots surrounded by circles) FG method eigenfunctions. Picture taken from C. Clay Marston and Gabriel G. Balint-Kurti *The Fourier grid Hamiltonian method for bound state eigenvalues and eigenfunctions*. *J.Chem.Phys.***91**, 3571,(1989).

6 Examples

As an example comparing some of the methods, we take the Morse potential. First example (C. Clay Marston and Gabriel G. Balint-Kurti[5]) compares the bound state eigenvalues and eigenfunctions computed from the diagonalization of the Hamiltonian constructed by the help of the FG method with the eigenvalues and eigenfunctions which are the result from the analytical solution to the Morse curve problem. In the second example (C. Leforstier et. al.[9]) different time propagation methods are compared. In both examples we are considering H_2 . The Morse potential is defined by

$$V(x) = D(1 - e^{-\alpha(x-x_e)})^2 \quad (195)$$

The parameters used are those applicable to H_2 and for numerical values of these parameters see (C. Clay Marston and G. Balint-Kurti[5]). The first example studied has 129 grid points and the vibrational quantum number is $v = 15$. In figure(1) the analytic solution is represented by a solid line and the numerically computed by dots surrounded by circles. In the C. Clay Marston and Balint-Kurti[5] paper the wavefunction is superimposed on the scaled Morse potential curve. The zero of the wave functions is at the bound state energies. The analytic solution is scaled so that it will coincide with the numerically computed values when they are at their maximum. The normalization condition $\sum_i |\psi_i|^2 = 1$ has been used.

In C. Leforstier et. al.[9] four methods are used: The SOD method, The split

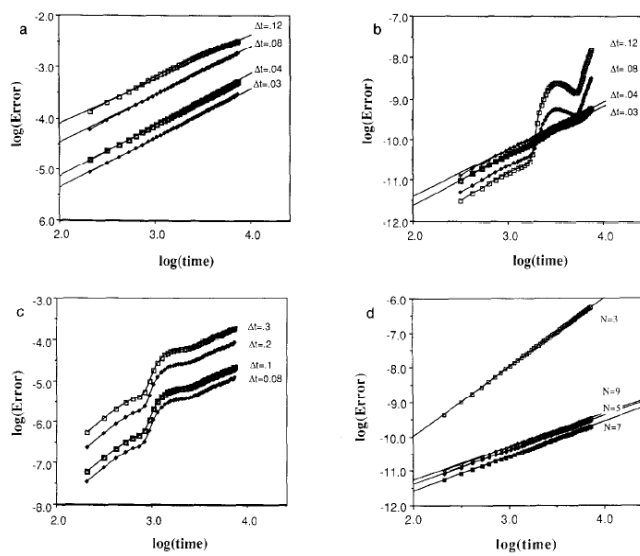


Figure 2: (a) SOD initial scattering state.(b) SPO bound initial state. (c) SPO scattering initial state. (d) SIL bound initial state. Picture taken from C. Leforstier et. al. *A comparison of different propagation schemes for the time dependent Schrödinger equation. J.Comput.Phys***94**, 59(1991)

operator method(SPO), the short iterative Lanczos method (SIL) and finally the Chebyshev method (CH). The methods are not always interchangeable but in the problem we are considering all four methods are applicable. In this example a time independent Hamiltonian is used. A grid with $N = 256$ points and $\Delta x = 0.10$ was used. For the generators of the reference wavefunction a time step of $\Delta t = 12.0$ was chosen. We also have $N_{times} = 7000$. For the numerical values of the parameters see (C. Leforstier et. al. [9]). Two initial states were used for the calculations. First a scattering event which was simulated by placing the initial wavefunction in the asymptotic region where we have negative average momentum. In the simulation a Gaussian wavefunction was used. This allowed the wavefunction frequency ω_w to change by varying the wavefunctions width. Second a completely bound wave function was simulated. This wavefunction oscillates in the bound part of the potential. The first series of computations studied the accumulated error for the different methods. In the figures this error is shown as a function of time. When it comes to comparison, the fact that the Chebyshev method has a constant time scaling error must be taken into account. For the parameters of the scattering state and of the bound state, see (Leforstier et. al.[9]). In figure 2(a) we have the logarithm of the accumulated overlap amplitude error as a function of the logarithmic time for the SOD propagation method. We define the overlap error as $1 - |(\psi_{CH}(t), \psi_{SOD}(t))|$. The plot shows four different time steps: $\Delta t = 0.03, 0.04, 0.08$ and 0.12 . As a reference a Chebyshev wavefunction with a uniform error of 10^{-14} was used. A linear dependence with respect to the accumulated error is observed, which should be the case with a stepwise integrator. The convergence of the method is shown in the graph. In figure 2(b), we have the logarithm of the accumulated amplitude error as a function of the logarithmic time for the SPO method. The error calculations are analogous to the one in figure 2(a). The initial condition is in correspondence to a bound state. The behavior of the convergence is as seen different from the SOD method. We have that the large time step calculations display an oscillatory behavior with respect to time. This comes from the fact that the commutation relation shows a non-uniform behavior as a function of the wavefunctions average position. The source of the error in the SPO method is that higher order commutators are neglected. As can be seen, the converged results show a linear accumulation of error with respect to time. In figure 2(c), we have the overlap phase error for the scattering initial state calculations for the split operator method. The phase error is defined as the phase of the overlap $(\psi_{CH}(t), \psi_{SPO}(t))$. Four time steps were used $\Delta t = 0.08, 0.1, 0.2$ and 0.3 . For all the four times step a nonlinear dependence is seen. In figure 2(d), we have the overlap phase error as a function of the logarithmic time for the bound initial state for the SIL propagation. The four plots show the result for the orders 3, 5, 7 and 9 of the interpolating polynomial over the fixed time step. We can see that for the polynomials of orders 5,7 and 9 there is a linear dependence which was expected. But for the polynomial of order 3 there is a accumulation of the quadratic overlap amplitude error. When higher orders are used the error saturates quickly. The Chebyshev method has a constant error scaling with time which should be mentioned for comparison reasons.

The next series of computations in C. Leforstier et. al. [9] evaluated for the fixed total propagation time is the scaling of error. In figure 3(a), we have the logarithm of the amplitude error as a function of the logarithm of the number of FFT calls at a fixed time for the SOD propagation. The four times used

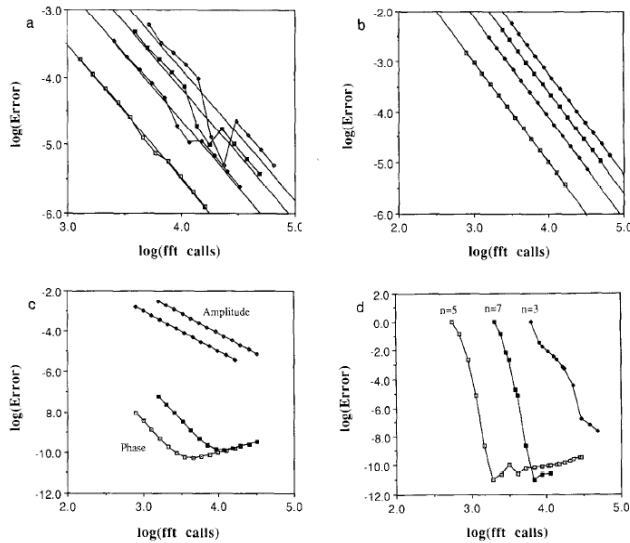


Figure 3: (a) SOD bound initial state. (b) SPO bound initial state. (c) SPO bound initial state. (d) SIL bound initial state. Picture taken from C. Leforstier et. al. *A comparison of different propagation schemes for the time dependent Schrödinger equation. J.Comput.Phys***94**, 59(1991)

for the bound initial state where 600, 1200, 1800 and 2400 a.u.(a.u. stands for atomic units). The earliest time is in the leftmost plot. It is seen that for the linear fits there is an approximate slope of -2 and the accumulation of the fixed error in time is like $t^{3/2}$. One thing noted is that the error has a cubic dependence upon numerical effort. This holds for the initial states, the amplitude and phase errors. Figure 3(b) is the same as figure 3(a) but for the split operator propagator phase error. In this case the linear fits also have a slope of -2. The result was the expected one since this is a second-order method. That it is a second-order method can also be seen from that there is a quadratic convergence of the error with respect to numerical effort. In figure 3(c), a comparison between the phase and amplitude error is displayed for the SPO propagator for 600 and 2400 atomic time units. The lower plots shows the amplitude error, the upper plots shows the phase error. Figure 3(d) is the same as figure 3(a) but for the SIL propagator amplitude error. The polynomial orders used for the result for 2400 atomic time units were 3, 5 and 7. The plot shows the convergence for the SIL propagation method for these three orders. It is seen that we have no simple linear relation which fits the data. It is also so that with numerical effort the error saturates which indicates that we have an accumulation of the round-off errors in the SIL method. In figures 4(a) and 4(b). The phase error dependence of the SPO propagator and the SIL propagator as a function of time is shown and we use a fifth-order interpolating polynomial. As a function of time for the initial scattering state wave function the width of the initial wavefunctions denoted as σ was 0.15, 0.20, 0.25 and 0.30. The time step was 0.04 a.u.. The Lanczos phase error is as seen sensitive when it comes to the choice of initial state. This is not the case when it comes to the split-operator.

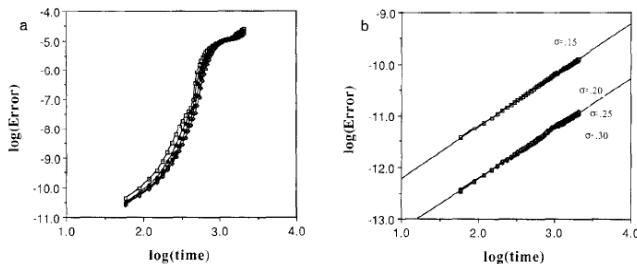


Figure 4: (a) Phase error dependence of the SPO propagator. (b) Phase error dependence of the SIL propagator. Picture taken from C. Leforstier et. al. *A comparison of different propagation schemes for the time dependent Schrödinger equation. J.Comput.Phys***94**, 59(1991)

For the amplitude error the two methods display similar behavior. The phase error as a function of time for three of the methods with bound initial state condition is shown in figure 5. The phase error as a function of numerical effort at a fixed time of 2400 a.u. for the four methods is shown in figure 6. The bound initial conditions are used and with the help of the number of FFT calls the numerical effort is measured..

The next example we are going to take up is the scattering of a wavepacket. The paper I´m referring to is (Iitaka[8]). The methods he is comparing are the Crank-Nicholson method, Chebyshev method, MSD2 method or SOD method, MSD4 method and MSD6 method. MSD4 and MSD6 are extensions of MSD2 (for details see Iitaka[8]). The example we will study is the scattering of a wavepacket. The object considered is the Hamiltonian of an electron in one dimension, $H = \frac{p^2}{2} + V(x)$ where $V(x)$ is the static potential. When it comes to the case of scattering of a wavepacket, there exists no exact solution. So we use the solution produced by the Chebyshev method instead. The error of the phase is then not available for the Chebyshev method. The parameters used for the grid are $\Delta x = 1$ and $N = 100$. For the scattering potential, we have

$$V(x_i) = \begin{cases} V_0 = 0.2, & x_L = 45 \leq x_i \leq x_R = 55 \\ 0 & otherwise \end{cases}$$

for the parameters of the wavefunction see (Iitaka[8]). As an initial wave function we have a Gaussian wave packet and the initial auxiliary wavefunctions at $t = \Delta t, 2\Delta t, \dots$, which we need to start the SOD propagation are created by using the time evolution operator Taylor expansion. In figure 7(a) and 7(b) we see the phase error in the scattering of a wave packet as a function of the dimensionless time $E_c t$. In 7(a) we have $\alpha = 0.1$ and in 7(b) we have $\alpha = 0.01$, where α is the dimensionless time step. In figure 8(a) and (b) we see the norm error $\epsilon_{norm} = | \langle \phi, t | \phi, t \rangle - 1 |$ in the scattering of a wavepacket as a function of the dimensionless time $E_c t$. In 8(a) the dimensionless time step is $\alpha = 0.1$ and in 8(b) $\alpha = 0.01$.

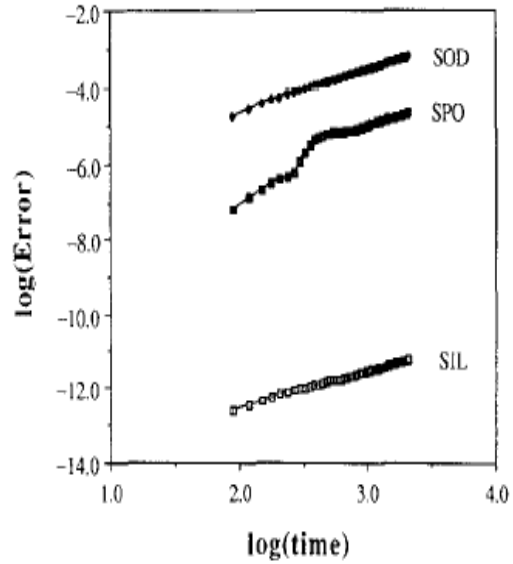


Figure 5: A comparison of the phase error as a function of time for three propagators with bound initial state condition. Picture taken from C. Leforstier et. al. *A comparison of different propagation schemes for the time dependent Schrödinger equation. J.Comput.Phys***94**, 59(1991)

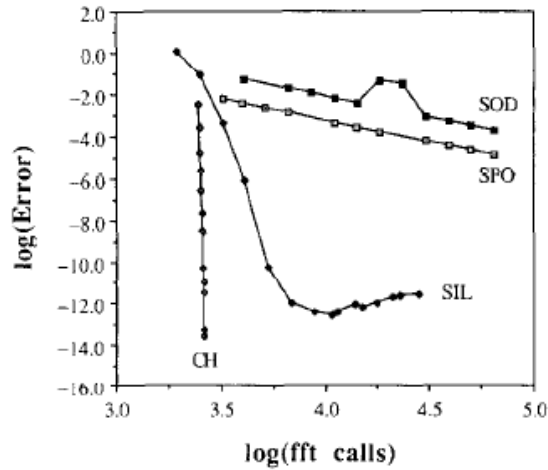


Figure 6: Phase error as a function of numerical effort for the four methods. Picture taken from C. Leforstier et. al. *A comparison of different propagation schemes for the time dependent Schrödinger equation. J.Comput.Phys***94**, 59(1991)

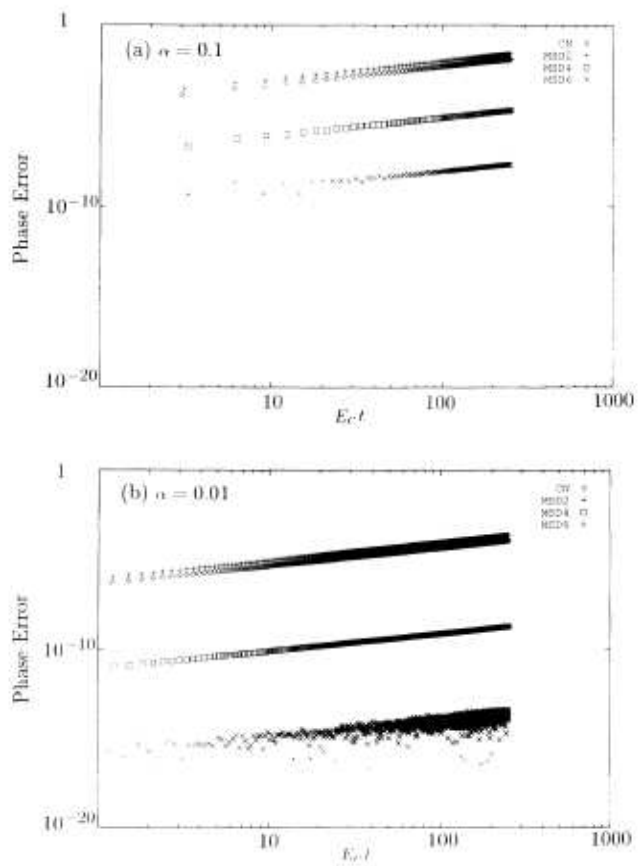


Figure 7: Phase error in the scattering of a wavepacket. The dimensionless time step is (a) $\alpha = 0.1$ and (b) $\alpha = 0.01$. Picture taken from Toshiaki Iitaka *Solving the time-dependent Schrödinger equation numerically. Phys.Rev. E49*, 59(1991)

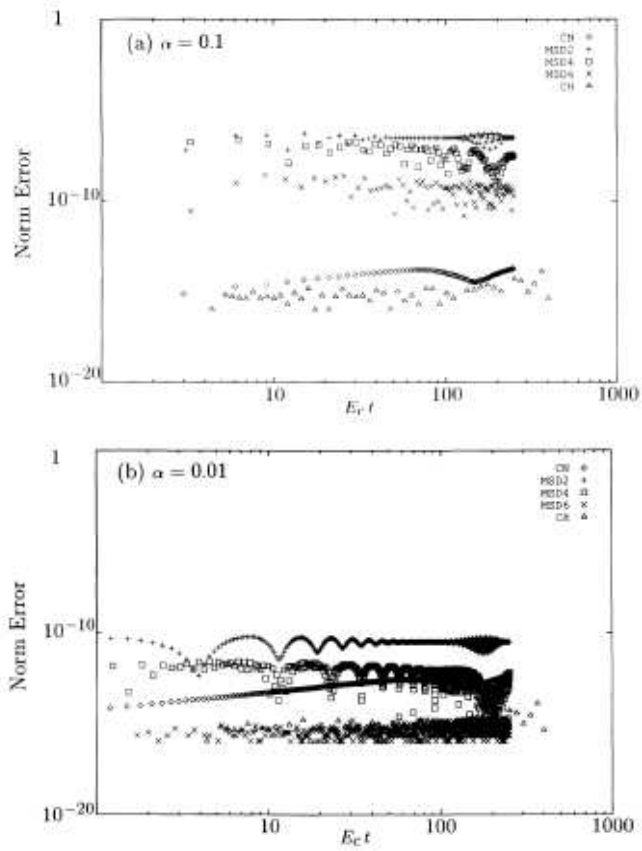


Figure 8: Norm error in the scattering of a wavepacket. The dimensionless time step is (a) $\alpha = 0.1$ and (b) $\alpha = 0.01$. Picture taken from Toshiaki Iitaka *Solving the time-dependent Schrödinger equation numerically. Phys.Rev. E49, 59(1991)*

7 Summary

As mentioned several times in this thesis only a few problems concerning time-dependent Schrödinger equations can be solved analytically. So numerical methods must be used. We have that the formal framework for quantum mechanics is an infinite-dimensional Hilbert space. We projected this space onto an N -dimensional space by the use of projection operators. We described the different representations of the basis functions, a spectral and a pseudospectral representation. In other words we studied the spatial part of the problem. We continued by the temporal part, where we discussed time propagation and the different methods for this purpose. A comparison between some of the different methods is summarized in the following way, where we compare stability, norm, energy, error type, error scaling, Hamiltonian and storage arrays (LeForstier et.al.[9])

SPO	SOD	Chebyshev	Lanczos
Stable	Unstable	Unstable	Stable
Unitary	Unitary	Not unitary	Unitary
Not conserved	Conserved	Not conserved	Conserved
Quadratic	Quadratic	Exponential	High order
No mixed terms	No restriction	Time independent	No restriction
2	3	4	Order+1

When it comes to error type for the different methods the following results are achieved(LeForstier et. al.[9]). The Lanczos and Chebyshev method: have arbitrary accuracy and the split-operator method(SPO) has commutator accuracy and finally the SOD method has an error type of $(E_n/\Delta t)^3$. We now mention some results considering the different methods. First the Chebyshev method; this method has no accumulated error and the amplitude and phase error are approximately of equal size. One negative thing with the Chebyshev method is that the intermediate wave functions are not available. When it comes to stepwise functions like the SOD method and Crank-Nicholson method they produce the wave function at each step. The split-operator method, the SOD method and the Chebyshev method have been successfully used when it comes to multidimensional problems and non-Cartesian coordinate choices. Some final comments can be made: For time-independent Hamiltonian operators would the Chebyshev method be the best choice, because of its exponential convergence, flexibility and accuracy. For time-dependent Hamiltonian operators the Lanczos method is the best choice, because it provides good accuracy and efficiency for a wide class of potentials.

8 Appendix

8.1 Orthogonal polynomials

Definition 8.4.1(Schatzman[14])

We call the sequence of polynomials $P_0, P_1, \dots, P_n, \dots$ orthogonal relative to a weight w , which is strictly positive almost everywhere and integrable on an interval $[a, b]$ if it has the following properties:

- (a) For any n , P_n is of degree n and the coefficient of its term of degree n is 1.
- (b) For any n , P_n is orthogonal to P_{n-1} , that is, all the polynomials of degree strictly less than n . The orthogonal polynomials are ordered from number zero and the n -th orthogonal polynomial is always of degree n .

We call the normalized polynomials

$$\hat{P}_n = \frac{P_n}{\|P_n\|} \quad (196)$$

orthonormal to a weight w .

Theorem 8.4.2(Schatzman[14])

For any weight w , which is integrable on the closed bounded interval $[a, b]$, there exists a sequence of orthogonal polynomials satisfying definition (8.4.1.). If

$$P_n = X^n - \sum_{i=0}^{n-1} c_{in} P_i \quad (197)$$

then

$$c_{in} = \frac{(X^n, P_i)}{(P_i, P_i)} \quad (198)$$

By using these relations we can determine the coefficients of orthogonal polynomials relative to a weight w on an interval $[a, b]$ by quadrature.

Theorem 8.4.3(Schatzman[14])

Let w be a weight which is integrable and strictly positive almost everywhere on the compact interval $[a, b]$. Then, for all $n \geq 1$, the orthonormal polynomials P_{n+1}, P_n and P_{n-1} are linked by the following recurrence relation:

$$P_{n+1} = (A_n x + B_n) P_n - C_n P_{n-1}, \quad (199)$$

where the constants A_n, B_n and C_n depend only on the polynomials P_{n+1}, P_n and P_{n-1} .

8.2 Chebyshev polynomials

We define the Chebyshev polynomials of the first kind by the following recurrence relation

$$T_{n+1}(x) = 2xT_n(x) - T_{n-1}(x) \quad (200)$$

where $T_0(x) = 1$ and $T_1(x) = x$.

The usual generating function for T_n is

$$\sum_{n=0}^{\infty} T_n(x)t^n = \frac{1-tx}{1-2tx+t^2}. \quad (201)$$

and the exponential generating function is

$$\sum_{n=0}^{\infty} T_n(x) \frac{t^n}{n!} = \frac{1}{2} (e^{(x-\sqrt{x^2-1})t} + e^{(x+\sqrt{x^2-1})t}). \quad (202)$$

We define the Chebyshev polynomials of the second kind by the following recurrence relation

$$U_{n+1}(x) = 2xU_n(x) - U_{n-1}(x) \quad (203)$$

where $U_0(x) = 1$ and $U_1(x) = 2x$. To give an example of a generating function for U_n , we have

$$\sum_{n=0}^{\infty} U_n(x)t^n = \frac{1}{1-2tx+t^2} \quad (204)$$

We can also define the Chebyshev polynomials by trigonometric functions. The Chebyshev polynomials of the first kind becomes

$$T_n(x) = \cos(n \arccos x) \quad (205)$$

so $T_n(\cos(v)) = \cos(nv)$ for $n = 1, 2, \dots$.

The polynomials of the second kind fulfill

$$U_n(\cos(v)) = \frac{\sin((n+1)v)}{\sin(v)} \quad (206)$$

A Chebyshev polynomial of first kind or second kind with degree n has n different simple roots denoted as Chebyshev roots, in the interval $[-1, 1]$. These roots are also denoted as Chebyshev nodes since these roots are used as nodes in polynomial interpolation. The Chebyshev roots of T_n are $x_k = \cos(\frac{(2k+1)\pi}{2n})$, for $k = 1, \dots, n$. The roots of U_n are $x_k = \cos(\frac{k\pi}{n+1})$, for $k = 1, \dots, n$. Both kinds of Chebyshev polynomials form a sequence of orthogonal polynomials. The polynomials of the first kind is on the interval $(-1, 1)$ orthogonal with respect to the weight $\frac{1}{\sqrt{1-x^2}}$. So we get:

$$\int_{-1}^1 \frac{T_n(x)T_m(x)}{\sqrt{1-x^2}} dx = \begin{cases} 0, & n \neq m; \\ \pi, & n = m = 0; \\ \pi/2, & n = m \neq 0; \end{cases}$$

The polynomials of the second kind is on the interval $(-1, 1)$ orthogonal with respect to the weight $\sqrt{1-x^2}$. So we get:

$$\int_{-1}^1 U_n(x)U_m(x)\sqrt{1-x^2} dx = \begin{cases} 0, & n \neq m; \\ \pi/2, & n = m; \end{cases}$$

The Chebyshev polynomials of the first kind fulfill the following discrete orthogonality condition:

$$\sum_{k=0}^{N-1} T_i(x_k)T_j(x_k) = \begin{cases} 0, & i \neq j; \\ N, & i = j = 0; \\ N/2, & i = j \neq 0; \end{cases}$$

where $x_k = \cos(\frac{\pi(k+1/2)}{N})$.

8.3 Discrete Fourier transforms

The discrete Fourier transform (DFT) is given by

$$U\left(\frac{n}{NT}\right) = \sum_{k=0}^{N-1} u(kT)e^{-2i\pi nk/N} \quad (207)$$

where $n = 0, 1, \dots, N-1$ and T is the sampling interval and N is the number of samples. The inverse discrete Fourier transform is given by

$$u(kT) = \frac{1}{N} \sum_{n=0}^{N-1} U\left(\frac{n}{NT}\right)e^{2i\pi nk/N} \quad (208)$$

where $k = 0, 1, \dots, N-1$. The DFT relates N samples of time with N samples of frequency by the help of the continuous Fourier transform. A fast Fourier transform (FFT) is an algorithm which computes the discrete Fourier transform and its inverse. We will now give an example to illustrate how the FFT algorithm works. The description will be an overview. (for a formal treatment see Brigham[5]). For simplicity and convenience we replace kT by k and n/NT by n . We have as before the DFT where we infer $W = e^{-i2\pi/N}$ so the DFT becomes

$$U(n) = \sum_{k=0}^{N-1} u_0(k)W^{nk} \quad (209)$$

where $n = 0, 1, \dots, N-1$. We choose the number of sample points N to be 4 and use the relation $W^{nk} = W^{nk \bmod(N)}$. The FFT algorithm has then the following expression in matrix form.

$$\begin{pmatrix} U(0) \\ U(1) \\ U(2) \\ U(3) \end{pmatrix} = \begin{pmatrix} 1 & 1 & 1 & 1 \\ 1 & W^1 & W^2 & W^3 \\ 1 & W^1 & W^0 & W^2 \\ 1 & W^3 & W^2 & W^1 \end{pmatrix} \begin{pmatrix} u_0(0) \\ u_0(1) \\ u_0(2) \\ u_0(3) \end{pmatrix}$$

The next step is the important one when it comes to the efficiency of the FFT algorithm. We factorize the matrix above in the following way.

$$\begin{pmatrix} U(0) \\ U(2) \\ U(1) \\ U(3) \end{pmatrix} = \begin{pmatrix} 1 & W^0 & 0 & 0 \\ 1 & W^2 & 0 & 0 \\ 0 & 0 & 1 & W^1 \\ 0 & 0 & 1 & W^3 \end{pmatrix} \begin{pmatrix} 1 & 0 & W^0 & 0 \\ 0 & 1 & 0 & W^0 \\ 1 & 0 & W^2 & 0 \\ 0 & 1 & 0 & W^2 \end{pmatrix} \begin{pmatrix} u_0(0) \\ u_0(1) \\ u_0(2) \\ u_0(3) \end{pmatrix}$$

One thing we can notice is that the results in the column vector to the left has been put in another order. We denote this new matrix as $\bar{\mathbf{U}}(\mathbf{n})$. We continue by letting

$$\begin{pmatrix} u_1(0) \\ u_1(1) \\ u_1(2) \\ u_1(3) \end{pmatrix} = \begin{pmatrix} 1 & 0 & W^0 & 0 \\ 0 & 1 & 0 & W^0 \\ 1 & 0 & W^2 & 0 \\ 0 & 1 & 0 & W^2 \end{pmatrix} \begin{pmatrix} u_0(0) \\ u_0(1) \\ u_0(2) \\ u_0(3) \end{pmatrix}$$

and finally we get

$$\begin{pmatrix} U(0) \\ U(2) \\ U(1) \\ U(3) \end{pmatrix} = \begin{pmatrix} u_2(0) \\ u_2(1) \\ u_2(2) \\ u_2(3) \end{pmatrix} = \begin{pmatrix} 1 & W^0 & 0 & 0 \\ 1 & W^2 & 0 & 0 \\ 0 & 0 & 1 & W^1 \\ 0 & 0 & 1 & W^3 \end{pmatrix} \begin{pmatrix} u_1(0) \\ u_1(1) \\ u_1(2) \\ u_1(3) \end{pmatrix}$$

For the computation of $\bar{\mathbf{U}}(\mathbf{n})$ by the help of the factorization we have to perform four complex multiplications and eight complex additions. For the computation of $\mathbf{U}(\mathbf{n})$ we have to perform sixteen complex multiplications and twelve complex additions. So in this example the number of multiplications are reduced with a factor of two. The time of computation is determined mainly by the number of multiplications. This can be said to give a picture of the efficiency of the FFT algorithm. One thing which must be taken care of is to change $\bar{\mathbf{U}}(\mathbf{n})$ so that we get $\mathbf{U}(\mathbf{n})$. This can be done in the following way: we rewrite $\bar{\mathbf{U}}(\mathbf{n})$ by instead of n use its binary equivalent. By changing in the following way 01 becomes 10 and 10 becomes 01 then $\bar{\mathbf{U}}(\mathbf{n})$ changes to $\mathbf{U}(\mathbf{n})$; (for details see Brigham[5]). Since we have that the difference between the inverse discrete Fourier transform and the discrete Fourier transform is a $1/N$ factor and opposite sign in the exponent, we can use a FFT algorithm for them both. So we get the same result if we evaluate the discrete Fourier transform from its definition or if we use an FFT to compute the discrete Fourier transform.

8.4 Morse potential

The Morse potential energy function is of the following form

$$V(r) = D_e(1 - e^{-a(r-r_e)})^2 \quad (210)$$

where $a = \sqrt{k_e/2D_e}$ and D_e is the well depth, k_e is the force constant at the minimum of the well, r is the distance between the atoms and r_e is the equilibrium bond distance. To express the stationary states on the Morse potential or in other words the solutions $\Psi(v)$ and $E(v)$ of the Schrödinger equation:

$$\left(-\frac{\hbar^2}{2m} \frac{\partial^2}{\partial r^2} + V(r)\right)\Psi(v) = E(v)\Psi(v) \quad (211)$$

we introduce the variables: $x = ar$; $x_e = ar_e$; $\lambda = \frac{\sqrt{2mD_e}}{a\hbar}$; $\epsilon_v = \frac{2m}{a^2\hbar^2}E(v)$. The Schrödinger equation becomes.

$$\left(-\frac{\partial^2}{\partial x^2} + V(x)\right)\Psi_n(x) = \epsilon_n\Psi_n(x) \quad (212)$$

where $V(x) = \lambda^2(e^{-2(x-x_e)} - 2e^{-(x-x_e)})$.

References

- [1] N.I. Akheizer and I.M. Glazman *Theory of Linear Operators in Hilbert Space*. Dover 1993
- [2] Karl Gustav Andersson and Lars-Christer Böiers *Ordinära differentialekvationer* Studentlitteratur 1989
- [3] David Bau III and Lloyd N. Trefethen *Numerical Linear Algebra*. SIAM 1997.
- [4] B.H. Bransden and C.J. Joachain *Quantum Mechanics second edition* Pearson 2000.
- [5] E. Oran Brigham *The Fast Fourier Transform* Prentice-Hall 1974.
- [6] C. Clay Marston and Gabriel G. BalintKurti *J.Chem.Phys.* **91**, 3571(1989).
- [7] Avner Friedman *Foundations of Modern Analysis* Dover 1970.
- [8] Toshiaki Iitaka *Phys. Rev. E* **49**, 4684(1994).
- [9] C. Leforestier et. al. *J. Comput. Phys.* **94**, 59(1991).
- [10] J.C. Light, I.P. Hamilton and J.V. Lill *J.Chem.Phys* **82**, 1400(1985).
- [11] R.G. Littlejohn et. al. *J. Chem. Phys.* **116**, 8691(2002).
- [12] Albert Messiah *Quantum Mechanics* Dover 1999.
- [13] J.J. Sakurai and J. Napolitano *Modern Quantum Mechanics second edition* Pearson 1994.
- [14] Michelle Schatzman *Numerical Analysis: a Mathematical Introduction* Oxford University Press 2002.
- [15] G.F. Simmons *Introduction to Topology and Modern Analysis* McGraw-Hill 1963.
- [16] H. TalEzer and R. Kosloff *J.Chem.Phys.***81**, 3967(1984)
- [17] David J. Tannor *Introduction to Quantum Mechanics: a Time-dependent Perspective* University Science Books 2007.
- [18] Jos M. Thijssen *Computational Physics second edition* Cambridge University Press (2007)
- [19] Claudio Verdozzi *The Lanczos Method* Unpublished.
- [20] Simon P. Webb and Sharon Hammes-Schiffer *J.Chem.Phys.* **113**, 5214(2000).